

**NASA TECHNICAL NOTE**



**NASA TN D-8510** *e.f.*

NASA TN D-8510

LOAN COPY: RE  
AFWL TECHNICAL  
KIRTLAND AFB.



**AN INVESTIGATION OF A CLOSE-COUPLED CANARD  
AS A DIRECT SIDE-FORCE GENERATOR ON  
A FIGHTER MODEL AT MACH NUMBERS  
FROM 0.40 TO 0.90**

*Richard J. Re and Francis J. Capone  
Langley Research Center  
Hampton, Va. 23665*





0134250

1. Report No. NASA TN D-8510		2. Government Accession No.		3. Recipient's Catalog No.	
4. Title and Subtitle AN INVESTIGATION OF A CLOSE-COUPLED CANARD AS A DIRECT SIDE-FORCE GENERATOR ON A FIGHTER MODEL AT MACH NUMBERS FROM 0.40 TO 0.90		5. Report Date July 1977		6. Performing Organization Code	
		8. Performing Organization Report No. L-11613		10. Work Unit No. 505-04-11-01	
7. Author(s) Richard J. Re and Francis J. Capone		11. Contract or Grant No.		13. Type of Report and Period Covered Technical Note	
9. Performing Organization Name and Address NASA Langley Research Center Hampton, VA 23665		14. Sponsoring Agency Code		12. Sponsoring Agency Name and Address National Aeronautics and Space Administration Washington, DC 20546	
		15. Supplementary Notes		16. Abstract  An investigation of the ability of a close-coupled canard positioned above the wing plane to act as a direct side-force generator on a fighter model has been conducted in the Langley 16-foot transonic tunnel at 0° angle of sideslip. The canard panels had 5° of dihedral and were deflected differentially or individually over an incidence range from 10° to -10° and a model angle-of-attack range from -4° to 15°. Mach number was varied from 0.40 to 0.90.  Significant side forces were generated by differential and single canard-panel deflections over the Mach number and angle-of-attack ranges. The yawing moment resulting from the forward location of the generated side force would necessitate a vertical tail/rudder trim force which would augment the forebody side force and be of comparable magnitude. Incremental side forces, yawing moments, lift, and pitching moments due to single canard-panel deflections were additive; that is, their sums were essentially the same as the forces and moments produced by differential canard-panel deflections of the same magnitude. Differential and single canard-panel deflections produced negligible rolling moments over the Mach number and angle-of-attack ranges.	
17. Key Words (Suggested by Author(s)) Direct side force Side-force generator Canard side force Close-coupled canard		18. Distribution Statement Unclassified — Unlimited  Subject Category 08			
19. Security Classif. (of this report) Unclassified	20. Security Classif. (of this page) Unclassified	21. No. of Pages 35	22. Price* \$4.00		

AN INVESTIGATION OF A CLOSE-COUPLED CANARD AS A  
DIRECT SIDE-FORCE GENERATOR ON A FIGHTER MODEL

AT MACH NUMBERS FROM 0.40 TO 0.90

Richard J. Re and Francis J. Capone  
Langley Research Center

SUMMARY

An investigation of the ability of a close-coupled canard positioned above the wing plane to act as a direct side-force generator on a fighter model has been conducted in the Langley 16-foot transonic tunnel at  $0^\circ$  angle of sideslip. The canard panels had  $5^\circ$  of dihedral and were deflected differentially or individually over an incidence range from  $10^\circ$  to  $-10^\circ$  and a model angle-of-attack range from  $-4^\circ$  to  $15^\circ$ . Mach number was varied from 0.40 to 0.90.

Significant side forces were generated by differential and single canard-panel deflections over the Mach number and angle-of-attack ranges. The yawing moment resulting from the forward location of the generated side force would necessitate a vertical tail/rudder trim force which would augment the forebody side force and be of comparable magnitude. Incremental side forces, yawing moments, lift, and pitching moments due to single canard-panel deflections were additive; that is, their sums were essentially the same as the forces and moments produced by differential canard-panel deflections of the same magnitude. Differential and single canard-panel deflections produced negligible rolling moments over the Mach number and angle-of-attack ranges.

INTRODUCTION

The pursuit of increased maneuverability for fighter aircraft has resulted in several aerodynamic and propulsion features which individually or in combination can produce uncoupled direct forces over a wide range of speeds and attitudes. Large direct lift forces can be generated by wing maneuver flaps (trailing-edge flaps) and engine thrust vectoring or by a combination of the two. Often, when these two features are combined, a canard (producing a positive lift increment) is used to trim the nose-down pitching moment from the wing flaps or vectored thrust (including pitching moment due to lift induced by super-circulation). A benefit of a canard-wing system for direct lift force is the ability to "point" the aircraft nose up or down (change angle of attack) while maintaining a constant lift coefficient.

Investigations of the longitudinal aerodynamic effects of different canard locations relative to the wing (refs. 1 to 4) indicate that at subsonic speeds,

a close-coupled canard positioned above the wing plane generally has the highest maximum lift capability and the most linear pitching-moment curves. Deflection of the canard for trim does not significantly increase the total lift of a configuration at low angles of attack because of the effect of the canard flow field on the wing (ref. 5). However, the stall angle of attack, and therefore the maximum lift capability, for the canard-wing combination is considerably greater than for the wing alone. In addition to offering increased trimmed-lift capability and possibly reduced trimmed drag at subsonic speeds, a close-coupled canard offers the potential for lower drag at supersonic speeds because of an improved progression of cross-sectional area.

Lateral-directional maneuverability above that possible by conventional means, such as ailerons, spoilers, asymmetric drag devices, vertical tails/rudders, and differential stabilizer deflections, can be provided by vertically mounted aerodynamic surfaces (direct side-force generators) ahead of the aircraft aerodynamic center. Side force produced by deflection of such a dedicated surface results in a yawing moment that can be trimmed with a vertical tail/rudder side force which augments the force produced by the forward control surface. With direct side-force capability, an aircraft can maintain a given flight direction and "point" its nose to either side (gun pointing) at a desired sideslip angle. Or, at the pilot's option, an aircraft can sideslip to a parallel flight path by a brief deflection of the side-force generator. Such maneuvering capabilities increase the effectiveness of an aircraft in aerial combat, tactical situations against fixed objectives, in-flight refueling, and cross wind landings (refs. 6 to 8). The aerodynamic characteristics of a swept-wing fighter model incorporating dedicated ventral direct side-force generators on the nose are presented in reference 9.

The present investigation was conducted to determine the ability of a close-coupled canard positioned above the wing plane for lift and trim at maneuver conditions to act also as a direct side-force generator. Differential deflection of the canard panels (or deflection of one panel) creates a nonsymmetric flow field about the forward fuselage which results in a side force that would be augmented by the required trim force on the vertical tail/rudder. Side-force generation in this manner provides the lateral-directional maneuverability offered by dedicated ventral direct side-force generators without the additional weight penalty or skin friction drag.

The investigation was conducted in the Langley 16-foot transonic tunnel at Mach numbers from 0.40 to 0.90, angles of attack from  $-4^{\circ}$  to  $15^{\circ}$ , and at an angle of sideslip of  $0^{\circ}$ . The model had a wing leading-edge sweep of  $50^{\circ}$ , a canard leading-edge sweep of  $45^{\circ}$ , a canard dihedral angle of  $5^{\circ}$ , and twin outboard vertical tails.

The left and right canard panels were deflected differentially at angles of  $\pm 5^{\circ}$  and  $\pm 10^{\circ}$ , and individually at angles of  $10^{\circ}$  and  $-10^{\circ}$ .

#### SYMBOLS

All aerodynamic coefficients are referenced to the body-axis system except lift and drag coefficients, which are referenced to the wind-axis system. The

moment reference center was located at a point 98.22 cm rearward of the fuselage nose and in the plane of the uncambered wing. (See fig. 1.) All dimensions presented are in the International System of Units (SI).

b	reference wing span, 102.48 cm
$C_D$	drag coefficient, $\frac{\text{Drag}}{qS}$
$C_L$	lift coefficient, $\frac{\text{Lift}}{qS}$
$C_l$	rolling-moment coefficient, $\frac{\text{Rolling moment}}{qSb}$
$C_{l\delta}$	rolling-moment coefficient due to differential canard deflection, $\frac{\Delta C_l}{\delta}$ , per degree
$C_m$	pitching-moment coefficient, $\frac{\text{Pitching moment}}{qS\bar{c}}$
$C_n$	yawing-moment coefficient, $\frac{\text{Yawing moment}}{qSb}$
$C_{n\delta}$	yawing-moment coefficient due to differential canard deflection, $\frac{\Delta C_n}{\delta}$ , per degree
$C_Y$	side-force coefficient, $\frac{\text{Side force}}{qS}$
$C_{Y\delta}$	canard effectiveness as a side-force generator, $\frac{\Delta C_Y}{\delta}$ , per degree
$\bar{c}$	wing mean geometric chord, 42.654 cm
$c_r$	root chord, measured streamwise
$c_t$	tip chord, measured streamwise
$\bar{c}_v$	vertical-tail mean geometric chord, 23.170 cm
$l_v$	longitudinal distance from model moment reference center to $\bar{c}_v/4$ , 37.17 cm
M	free-stream Mach number
q	free-stream dynamic pressure
S	reference wing area, 0.3808 m <sup>2</sup>
$\alpha$	angle of attack, deg
$\Delta$	increment in force or moment coefficient due to canard deflection

- $\delta$  total canard-panel deflection angle (difference in deflection angle between left and right canard panels),  $\delta_{c,Left} - \delta_{c,Right}$ , deg
- $\delta_c$  single canard-panel deflection angle, positive leading edge up, deg

#### DESCRIPTION OF MODEL

The general arrangement of the model and fuselage external contours are shown in figures 1 and 2, respectively. A photograph showing the sting-mounted model in the wind-tunnel test section is presented in figure 3.

The uncambered wing had an NACA 65A005 airfoil section at the wing-body juncture and varied linearly in thickness to an NACA 65A004 airfoil section at the wing tip. The wing had a leading-edge sweep of  $50^\circ$ , an aspect ratio of 2.759, a taper ratio of 0.2, and  $0^\circ$  dihedral.

The uncambered canard had an NACA 65A005 airfoil section at the canard-body juncture and varied linearly in thickness to an NACA 65A003 airfoil section at the tip. The canard had a leading-edge sweep of  $45^\circ$ , an aspect ratio of 2.506, a taper ratio of 0.376, and  $5^\circ$  dihedral when mounted on the model. The canard-panel axis of rotation was in a plane 66.68 cm rearward of the nose. The surface of the fuselage in the vicinity of the canard root was basically flat in the plane perpendicular to the canard axis of rotation (fig. 4), so that as the canard rotated, only a small gap occurred between the canard leading edge and the fuselage side. The ratio of exposed canard area to wing reference area was 0.1943, and the height of the canard above the wing reference plane at the model plane of symmetry was 0.121 $\bar{c}$ .

The fuselage represents that of a single-engine fighter aircraft having a chin inlet (faired over, see fig. 1) and a nozzle geometry representing an after-burning power setting. The inlet was faired over because the model was originally designed for high-pressure air propulsion-simulation testing with a support-strut mounting system beneath the nose. For the present investigation, the model was sting supported in the tunnel. The sting diameter was 6.35 cm at the model base.

#### TESTS AND CORRECTIONS

The investigation was conducted in the Langley 16-foot transonic tunnel, a single-return atmospheric wind tunnel with continuous air exchange. The slotted test section is octagonal in shape and measures 4.724 m between opposite walls (an area equivalent to a circle 4.85 m in diameter). The tunnel sting-support system pivots in such a manner that the model remains on or near the test-section center line throughout the angle-of-attack range.

The model was tested at Mach numbers from 0.40 to 0.90, at angles of attack from  $-4^\circ$  to  $15^\circ$ , and at a sideslip angle of  $0^\circ$ . Reynolds number, based on wing mean geometric chord, varied from  $3.4 \times 10^6$  at  $M = 0.40$  to  $5.6 \times 10^6$  at  $M = 0.90$ .

Aerodynamic forces and moments were measured by an internal six-component strain-gage balance. Model angle of attack was obtained by correcting the angle of the model support system for deflection of the sting and balance under aerodynamic loads and for test-section stream angularity. The force data are adjusted to the condition of free-stream static pressure at the fuselage base.

All configurations were tested with fixed boundary-layer transition on the model surfaces. The transition-fixing strips consisted of 0.25-cm-wide straight-line strips of No. 120 silicon carbide grit connecting points  $0.05c_r$  and  $0.10c_t$  aft of the leading edges of the wing, canard, and vertical tails. The transition strips on the ventral fins were located at a constant distance ( $0.05c_r$ ) from the leading edge. A transition band on the fuselage nose was located 2.54 cm rearward of the tip of the nose.

### PRESENTATION OF RESULTS

The data obtained in this investigation are presented in graphical form. An outline of the contents of the data and analysis figures is as follows:

	Figure
Effect of differential canard-panel deflection on model lateral aerodynamic coefficients . . . . .	5
Effect of differential canard-panel deflection on model longitudinal aerodynamic coefficients . . . . .	6
Effect of differential and single canard-panel deflection on model lateral aerodynamic coefficients . . . . .	7
Effect of differential and single canard-panel deflection on model lift and pitching-moment characteristics . . . . .	8
Effect of differential and single canard-panel deflection on model drag coefficient . . . . .	9
Variation with total canard deflection angle of aerodynamic-coefficient increments due to differential and single canard-panel deflection . . .	10
Variation with angle of attack of model lateral aerodynamic characteristics due to differential canard-panel deflection . . . . .	11
Variation with angle of attack of trimmed (calculated) side-force coefficient . . . . .	12

## DISCUSSION OF RESULTS

### Differential Canard-Panel Deflection

The lateral aerodynamic coefficients of the model with differential canard-panel deflections (fig. 5) show that significant levels of direct side force were generated over the angle-of-attack and Mach number ranges of this investigation. The yawing moment resulting from the side force generated by a forward control surface is in the direction such that the required vertical tail/rudder trim force would augment the forebody side force. For the configuration investigated and the moment reference center selected, the magnitude of the required trim force would be substantial. To illustrate this simply, calculations of trim increments were made by assuming that the vertical-tail force acted at one-quarter of the tail mean geometric chord  $\bar{c}_v/4$  and that the tail moment arm  $l_v$  was the distance between that point and the model moment reference center. The calculated increments are presented in figure 12 and were made from the following equation:

$$\Delta C_Y = \left[ (C_n \text{ for canard deflected}) - (C_n \text{ for canard at } 0^\circ) \right] \frac{b}{l_v}$$

However, the reader is cautioned that the total value of side-force coefficient shown in figure 12 is the result of a simple calculation, and the effects of sideslip angle on the model lateral aerodynamic characteristics and on the side-force-generating capabilities of the canard could not be considered here.

The effectiveness parameters for the generation of side force and yawing moment by differential canard deflection (fig. 5) are shown in figure 11(a) for  $\pm 5^\circ$  deflection and 11(b) for  $\pm 10^\circ$  deflection. The two figures indicate about the same side-force effectiveness level and variation with angle of attack. Yawing-moment effectiveness for  $\pm 10^\circ$  deflection was considerably less than for  $\pm 5^\circ$  deflection, although the variation with angle of attack was essentially the same.

Differential deflection of the canard panels produced negligible rolling moment (figs. 5 and 11). Apparently, the canard and wing flow fields interact in such a manner that the rolling moment on the differentially deflected canard panels is counteracted by an opposite rolling moment on the wing resulting from the canard wake.

Differential deflection of the canard panels had a negligible effect on model lift (fig. 6) at angles of attack up to about  $6^\circ$  but caused a slight decrease in lift-curve slope at the higher angles of attack, especially at Mach numbers of 0.80 and 0.90. Model longitudinal stability increased when the canard panels were differentially deflected, the greatest increase occurring at the lower Mach numbers. Zero-lift drag increased about 10 percent for  $\pm 5^\circ$  deflection and between 60 and 70 percent for  $\pm 10^\circ$  deflection.



## Single Canard-Panel Deflection

Deflection of a single canard panel was effective in the generation of significant side forces while producing negligible rolling moments (fig. 7). Negative (leading-edge down) deflection of a canard panel produced substantially greater side forces and yawing moments than an equal positive deflection. Comparison of the sums of the side-force and yawing-moment increments due to single panel deflections in opposite directions (dashed lines in fig. 7) indicates that the results are additive; that is, essentially the same forces and moments were measured for differential deflections of the same magnitude. The effect of angle of attack on the side-force-generating capabilities of single panel deflections is large in that, at  $14^\circ$  angle of attack, the upward (positively) deflected panel produces very little side force at a Mach number of 0.40 and negative side force at a Mach number of 0.90.

The lift and pitching-moment characteristics of the model for single canard-panel deflections (fig. 8) also indicate that the force and moment increments from single canard-panel deflections in opposite directions are additive. That is, essentially the same lift and pitching moment (dashed line in fig. 8) are obtained by adding single-panel increments as are measured for differential deflections of the same magnitude.

A minor instrumentation problem prevented acquisition of drag data with single canard-panel deflections to the same accuracy as with the differential deflections. However, accurate drag data for both canard panels deflected  $-5^\circ$ ,  $5^\circ$ ,  $10^\circ$  (not shown), and  $0^\circ$  and differentially deflected  $\pm 5^\circ$  and  $\pm 10^\circ$  have been used to adjust the drag polar levels of configurations with single panel deflections of  $10^\circ$  and  $-10^\circ$ . The data for both panels deflected  $-5^\circ$ ,  $0^\circ$ , and  $5^\circ$  were used to verify that drag increments due to canard deflection could be used to calculate the drag with differential canard deflection (the measured drag data for  $\pm 5^\circ$  deflection). Then, assuming that the drag increments were still additive for the larger canard deflections ( $10^\circ$ ), the data for canard deflections of  $0^\circ$ ,  $10^\circ$ , and  $\pm 10^\circ$  were used to calculate the minimum drag for the single canard-panel deflections. The experimentally determined drag polars for single canard-panel deflections were adjusted to the calculated minimum drag levels, so that only the minimum drag levels were changed and not the shape of the polars. (See fig. 9.)

What is most significant in figure 9 is the rotation of the model drag polars due to single canard-panel deflection. Downward deflection of a canard panel to  $-10^\circ$  increased the minimum drag, shifted it to a higher lift coefficient, and reduced the drag due to lift such that at lift coefficients of 0.3 and above, the drag was essentially the same as that with no canard deflection. If an optimized minimum drag were desired at some combined side-force and lift condition, the lateral and longitudinal trim-drag increments that would occur would have to be considered in order to determine the appropriate canard-panel deflections.

## Aerodynamic-Coefficient Increments

The variation of the aerodynamic-coefficient increments with total canard deflection angle is shown in figure 10. The symbols are not actual data points but were interpolated at even angles of attack from figures 5 to 8. In fairing the incremental data, only the data for differential canard deflection were considered.

Examination of the increments in figure 10 illustrates that single-panel increments are essentially additive for side force, yawing moment, lift, and pitching moment. It is also apparent that within the range of this investigation, the variation of side force with differential canard deflection is linear.

### SUMMARY OF RESULTS

An investigation of the ability of a close-coupled canard positioned above the wing plane to act as a direct side-force generator on a fighter model has been conducted at Mach numbers from 0.40 to 0.90 at  $0^\circ$  angle of sideslip. The canard panels had  $5^\circ$  of dihedral and were deflected differentially or individually in an incidence range from  $10^\circ$  to  $-10^\circ$  over a model angle-of-attack range from  $-4^\circ$  to  $15^\circ$ . The results of the investigation may be summarized as follows:

1. Significant side forces were generated by differential and single canard-panel deflections over the Mach number and angle-of-attack ranges investigated.
2. The yawing moment resulting from the forward location of the side force would necessitate a vertical tail/rudder trim force which would augment the forebody side force and be of comparable magnitude.
3. Incremental side forces, yawing moments, lift, and pitching moments due to single canard-panel deflections were additive; that is, their sums were essentially the same as the forces and moments produced by differential canard-panel deflection of the same magnitude.
4. Differential and single canard-panel deflections produced negligible rolling moments over the Mach number and angle-of-attack ranges investigated.

Langley Research Center  
National Aeronautics and Space Administration  
Hampton, VA 23665  
June 9, 1977

## REFERENCES

1. Gloss, Blair B.: Effect of Wing Planform and Canard Location and Geometry on the Longitudinal Aerodynamic Characteristics of a Close-Coupled Canard Wing Model at Subsonic Speeds. NASA TN D-7910, 1975.
2. Gloss, Blair B.: The Effect of Canard Leading-Edge Sweep and Dihedral Angle on the Longitudinal and Lateral Aerodynamic Characteristics of a Close-Coupled Canard-Wing Configuration. NASA TN D-7814, 1974.
3. Henderson, William P.: The Effect of Canard and Vertical Tails on the Aerodynamic Characteristics of a Model With a  $59^\circ$  Sweptback Wing at a Mach Number of 0.30. NASA TM X-3088, 1974.
4. Gloss, Blair B.: Effect of Canard Location and Size on Canard-Wing Interference and Aerodynamic-Center Shift Related to Maneuvering Aircraft at Transonic Speeds. NASA TN D-7505, 1974.
5. Gloss, Blair B.; and McKinney, Linwood W.: Canard-Wing Lift Interference Related to Maneuvering Aircraft at Subsonic Speeds. NASA TM X-2897, 1973.
6. Carlson, E. F.: Direct Sideforce Control for Improved Weapon Delivery Accuracy. AIAA Paper No. 74-70, Jan.-Feb. 1974.
7. Lockenour, J. L.; and Williams, W. G.: Stability and Control Potential for Future Fighters. The Effects of Buffeting and Other Transonic Phenomena on Maneuvering Combat Aircraft, AGARD-AR-82, July 1975, pp. 54-62, 201-207.
8. Hall, G. Warren: A Flight Test Investigation of Direct Side Force Control. AFFDL-TR-71-106, U.S. Air Force, Sept. 1971.
9. Capone, Francis J.: Effect of Direct Side-Force Generators on the Aerodynamic Characteristics of a Swept-Wing Fighter Model at Transonic Speeds. NASA TM X-2874, 1973.

Wing geometry

Mean geometric chord 42.654  
 Aspect ratio 2.759  
 Taper ratio 0.2  
 Airfoil sections:  
 Root (at body) NACA 65A005  
 Tip NACA 65A004

Canard geometry

Mean geometric chord 21.852  
 Aspect ratio 2.506  
 Taper ratio 0.376  
 Airfoil sections:  
 Root (at body) NACA 65A005  
 Tip NACA 65A003

Twin vertical tail geometry

Mean geometric chord 23.170  
 Taper ratio 0.231  
 Airfoil sections:  
 Root NACA 65A004  
 Tip NACA 65A003

Twin ventral fins

Airfoil section NACA 65A003

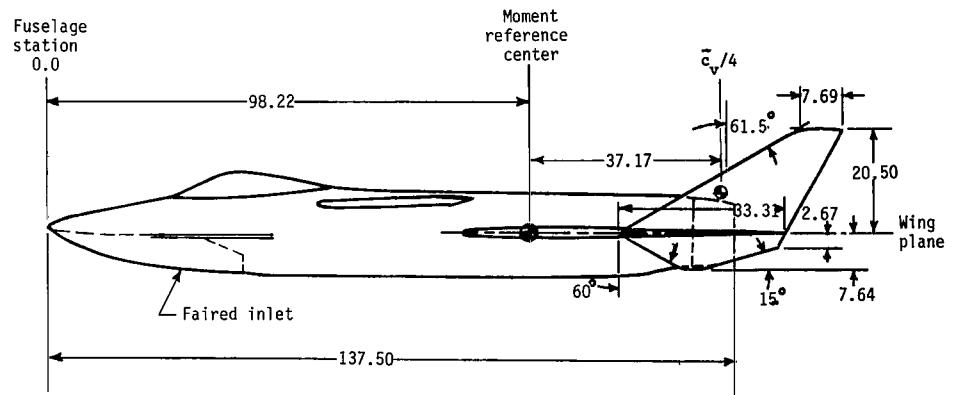
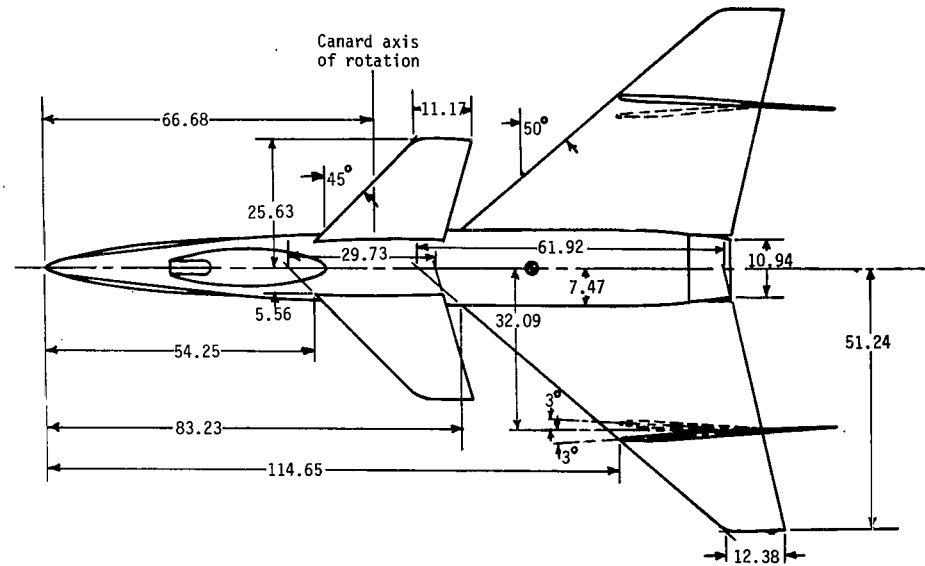
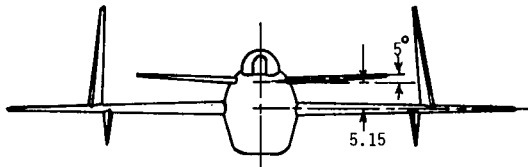


Figure 1.- General arrangement of model. (All dimensions are in centimeters unless otherwise indicated.)

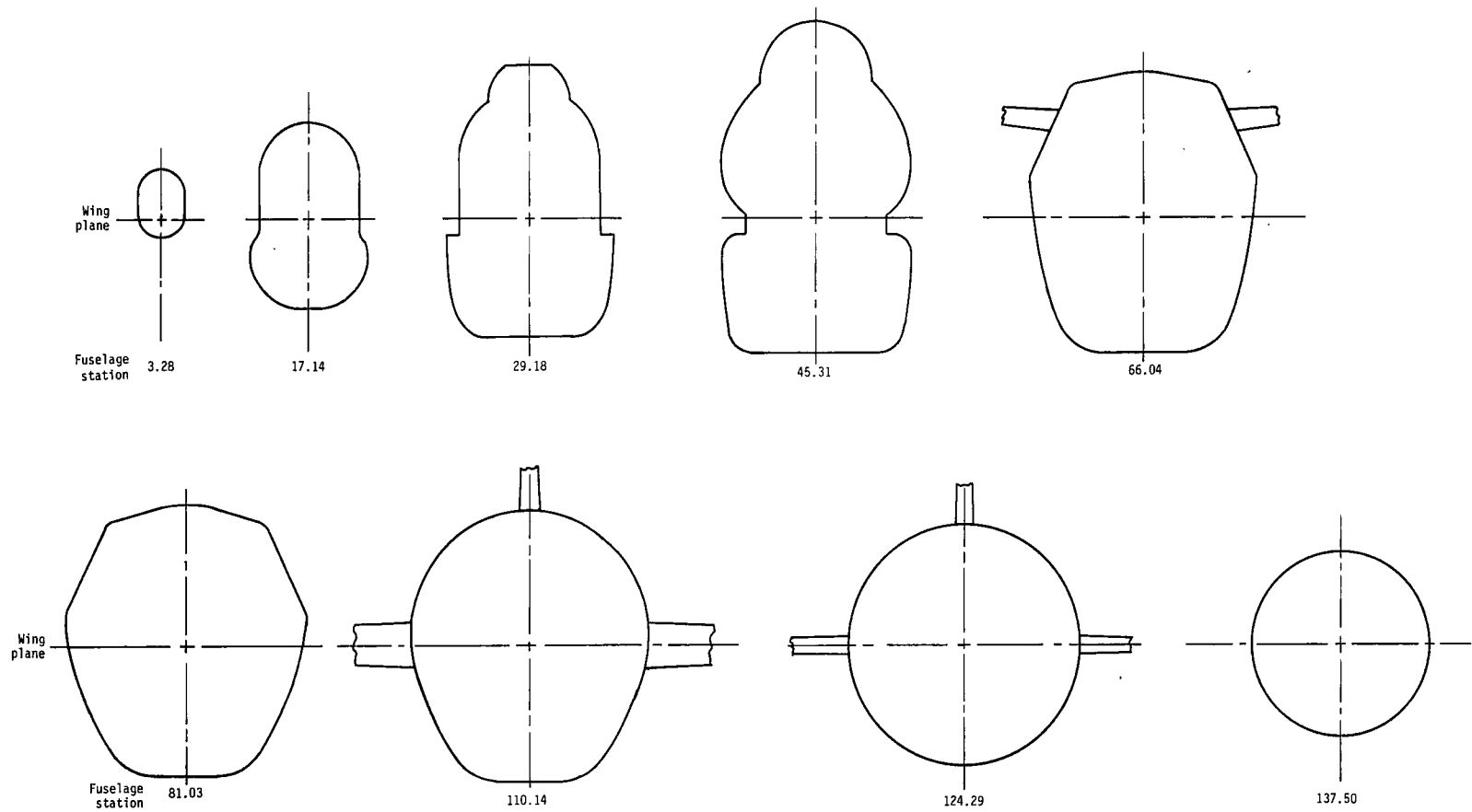


Figure 2.- Fuselage external contours. (All stations are in centimeters.)

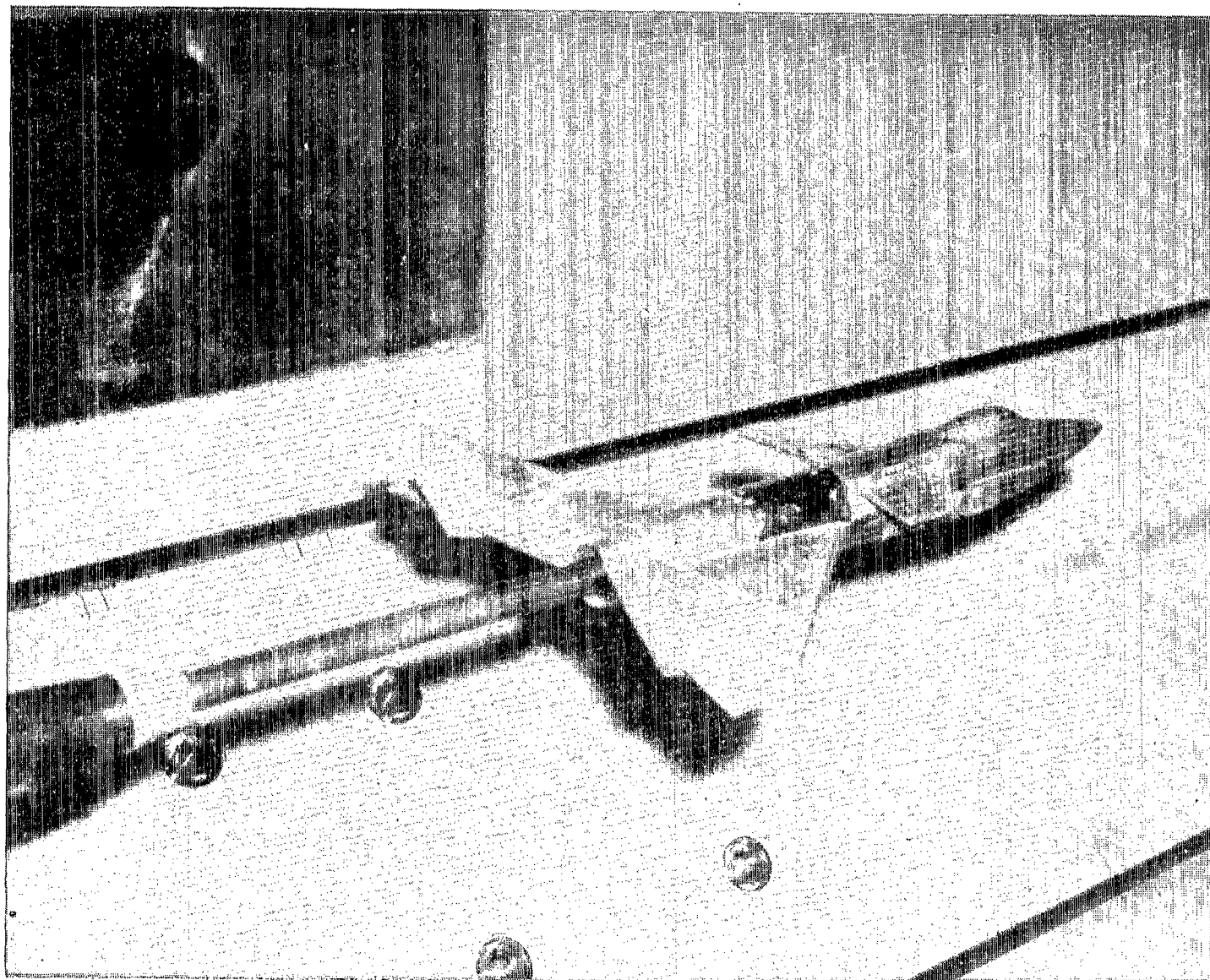


Figure 3.- Model mounted in wind-tunnel test section.

L-75-7712

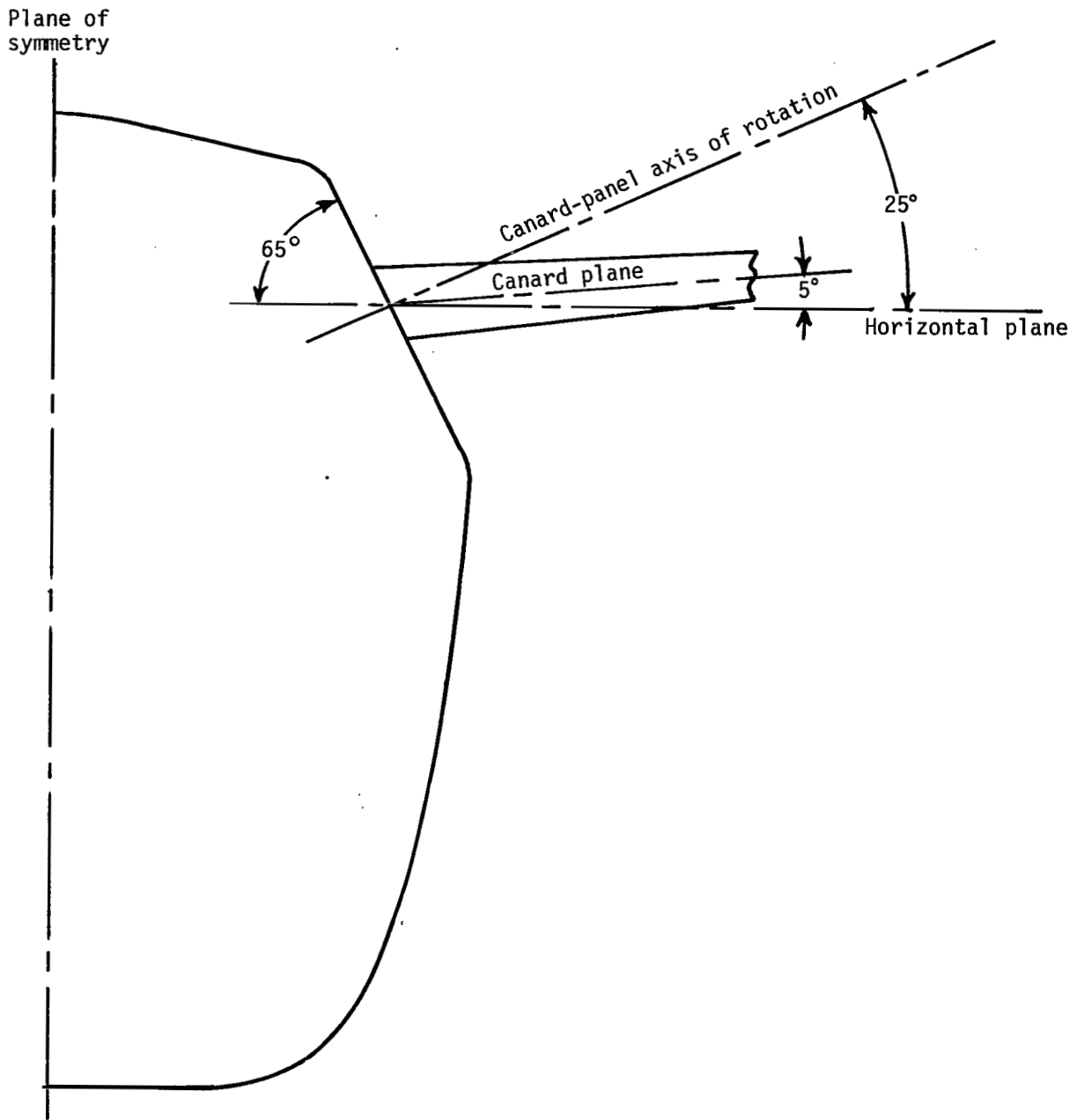
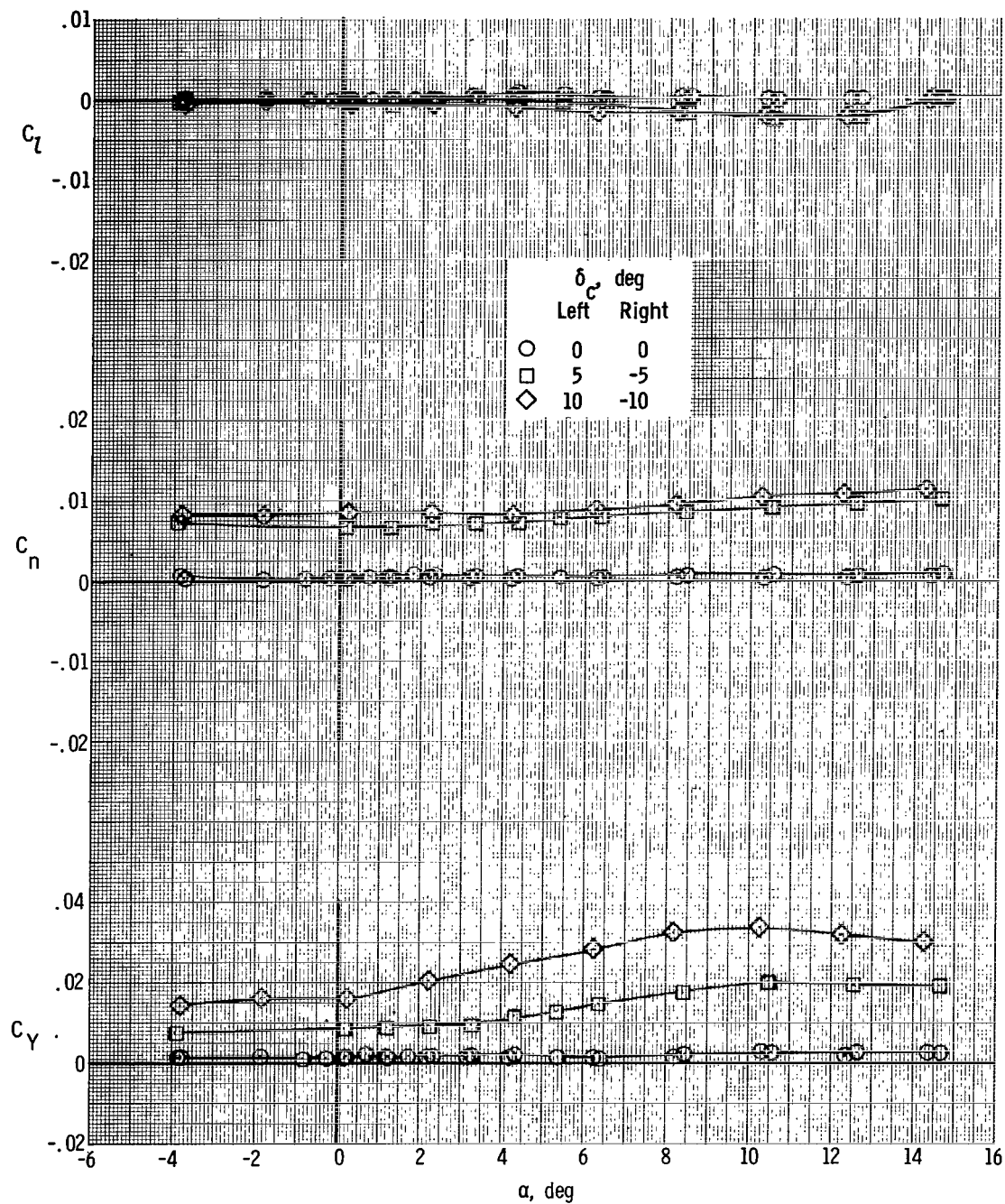


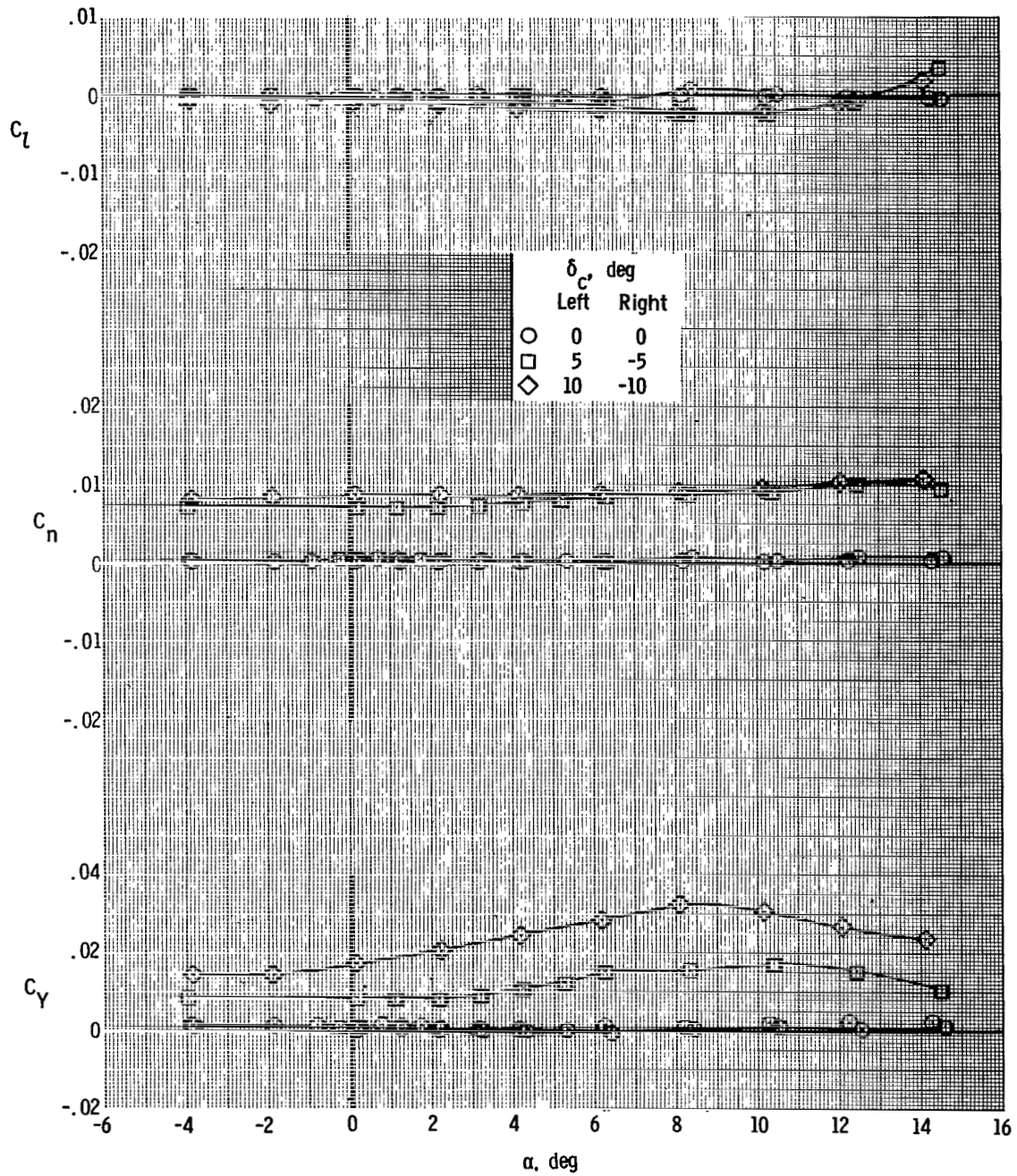
Figure 4.- Relative orientation of canard-panel axis of rotation to the canard plane.



(a)  $M = 0.40$ .

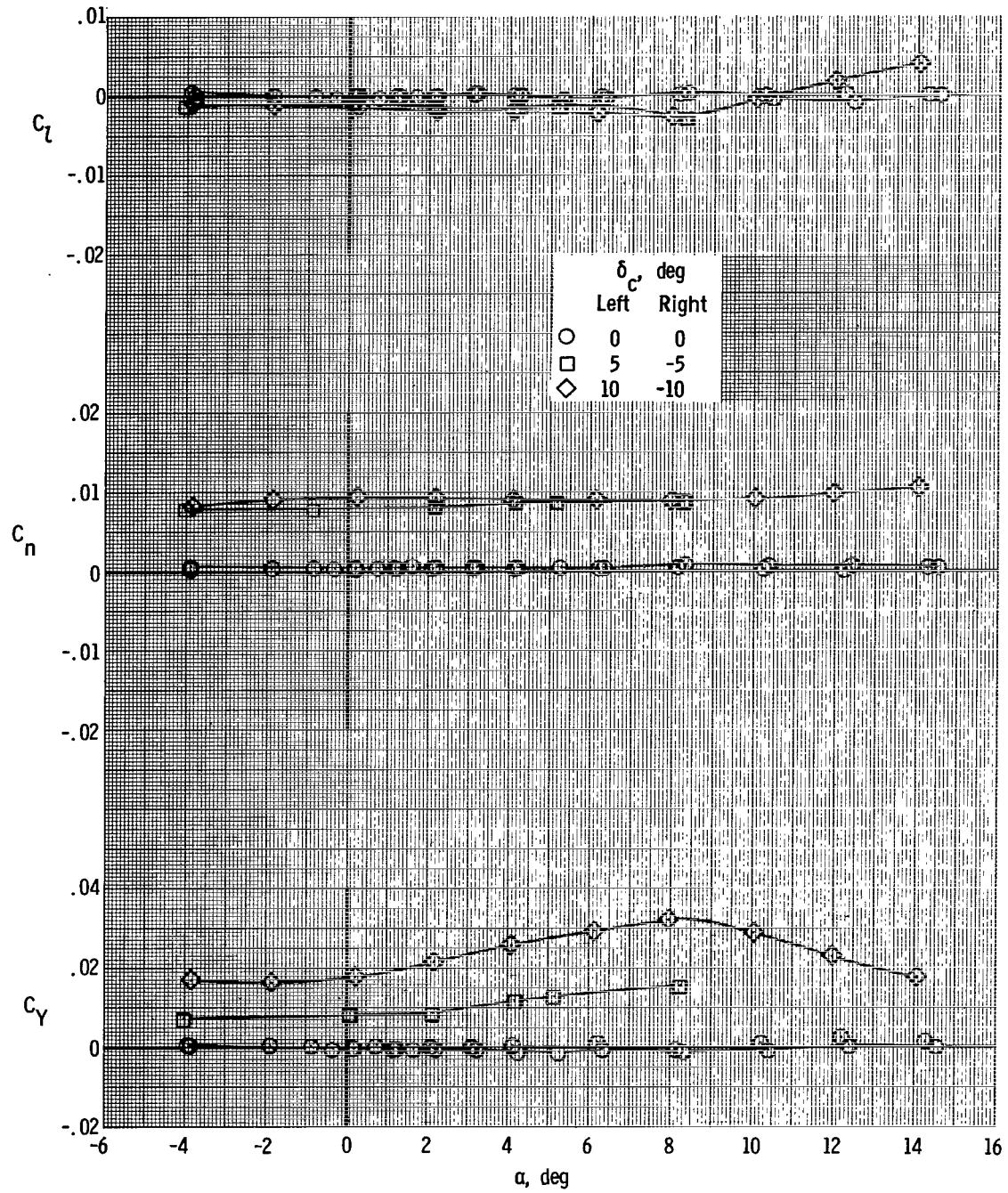
Figure 5.- Effect of differential canard-panel deflection on model lateral aerodynamic coefficients.





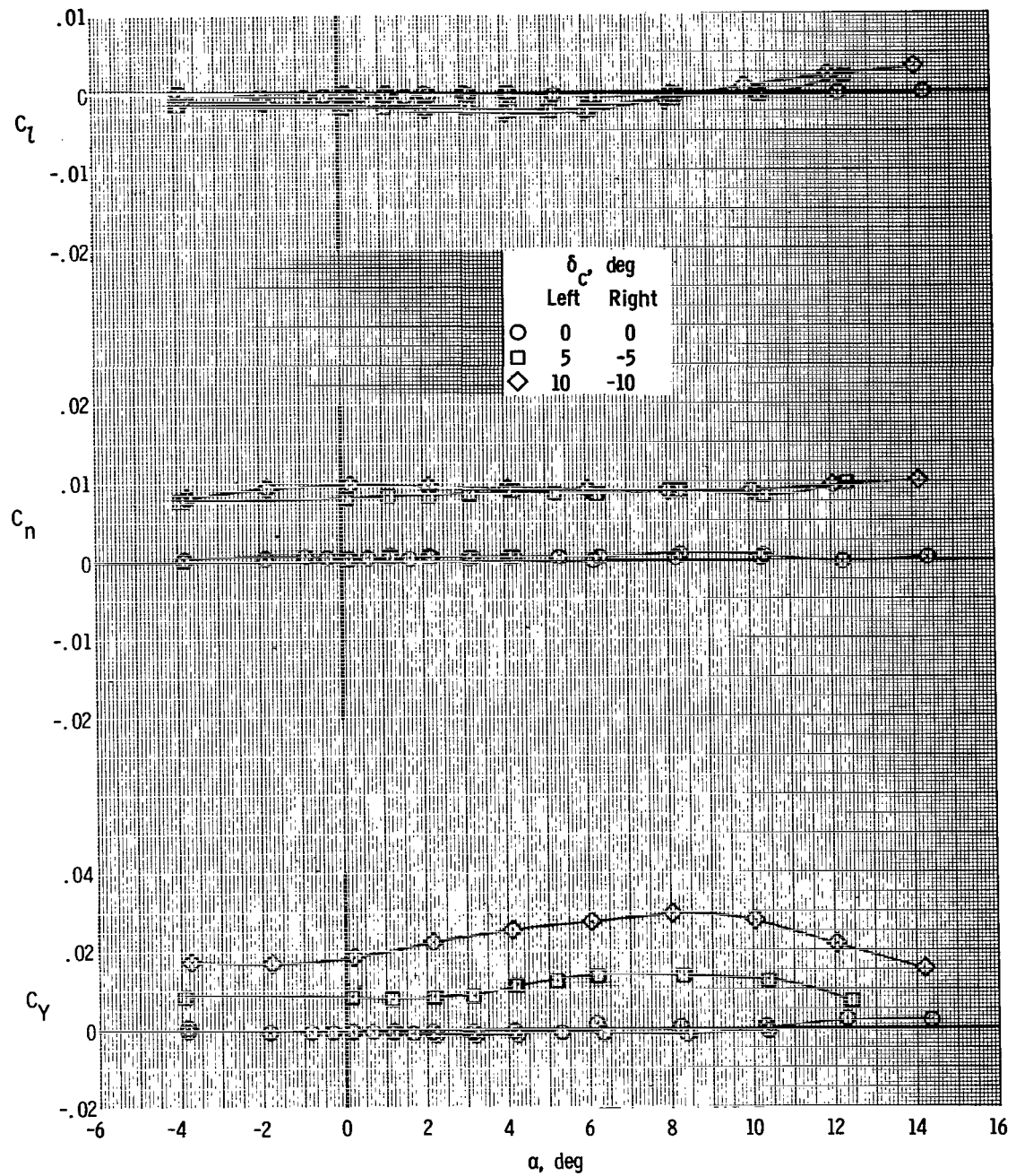
(b)  $M = 0.60$ .

Figure 5.- Continued.



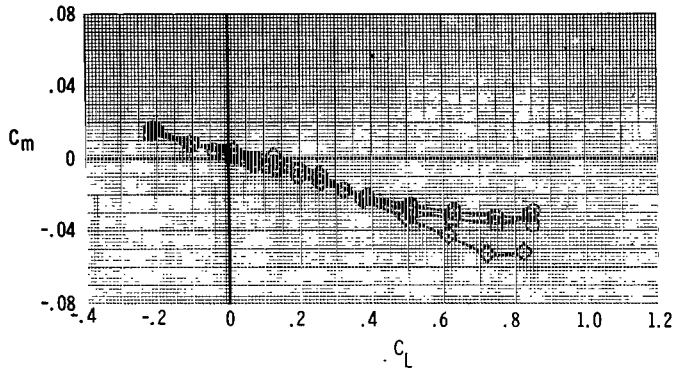
(c)  $M = 0.80$ .

Figure 5.- Continued.

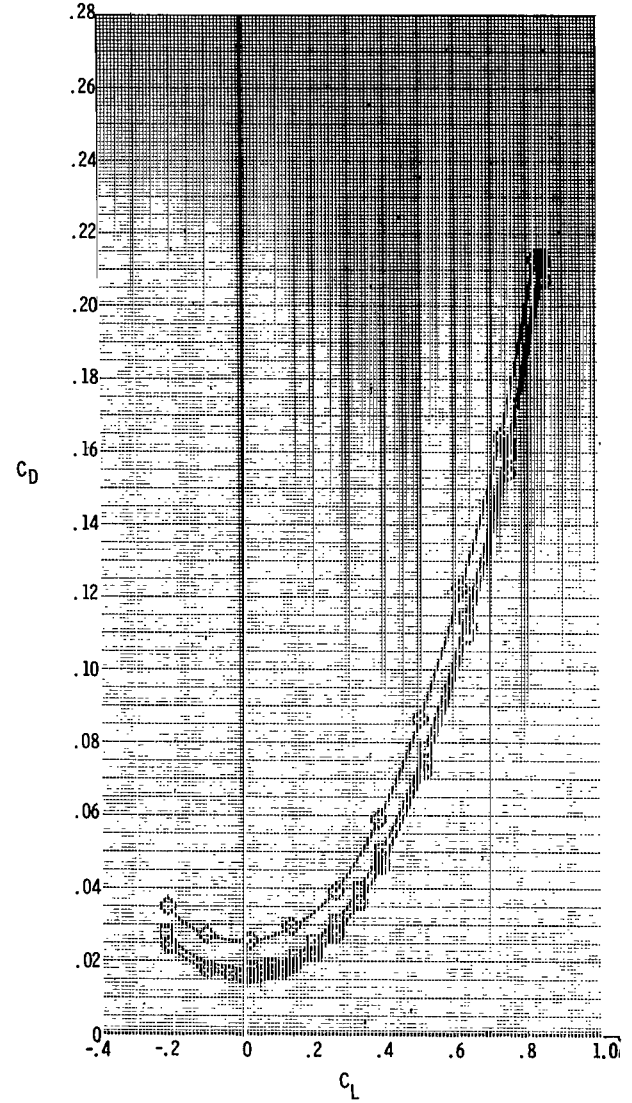
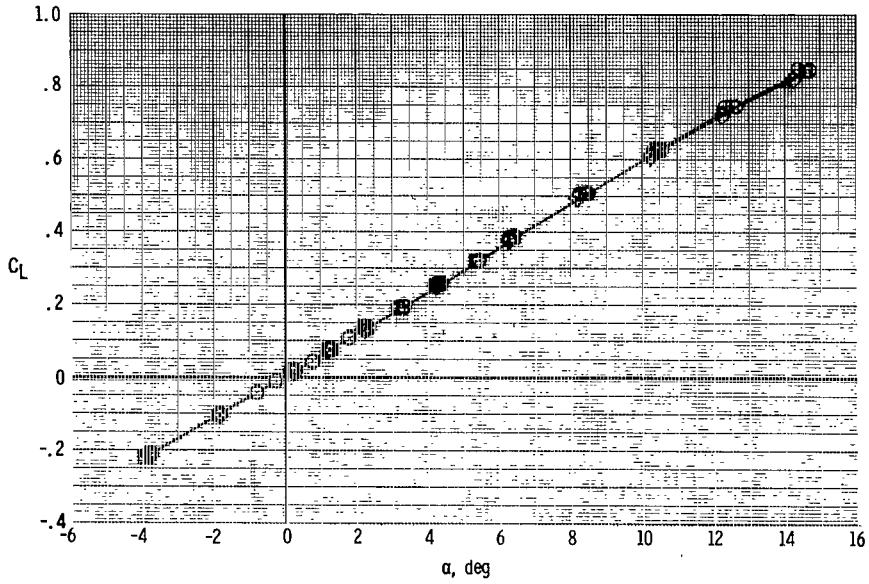


(d)  $M = 0.90$ .

Figure 5.- Concluded.

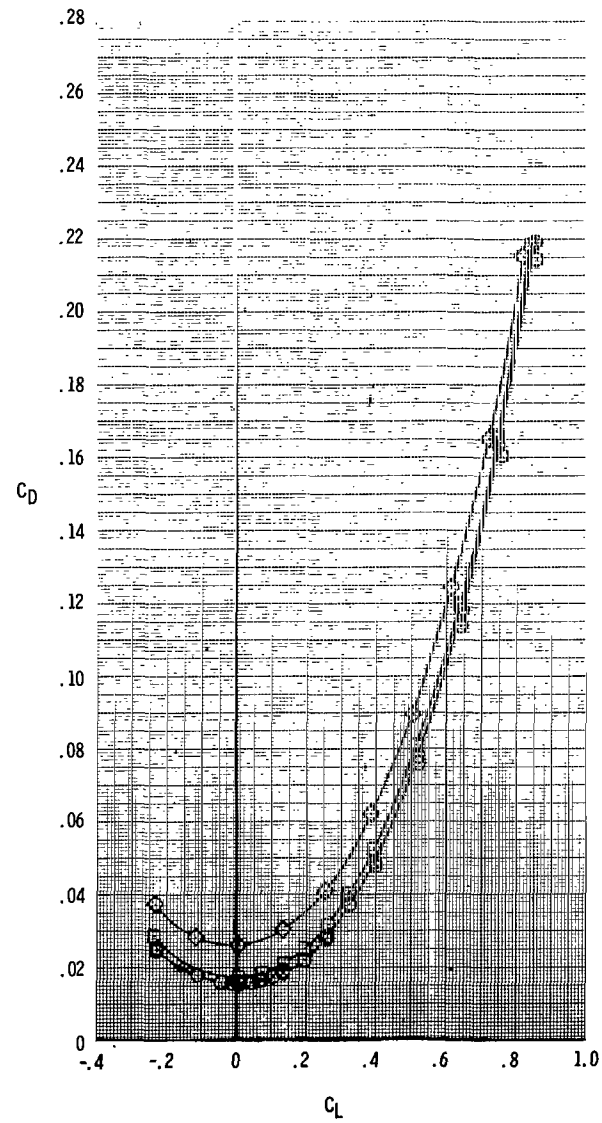
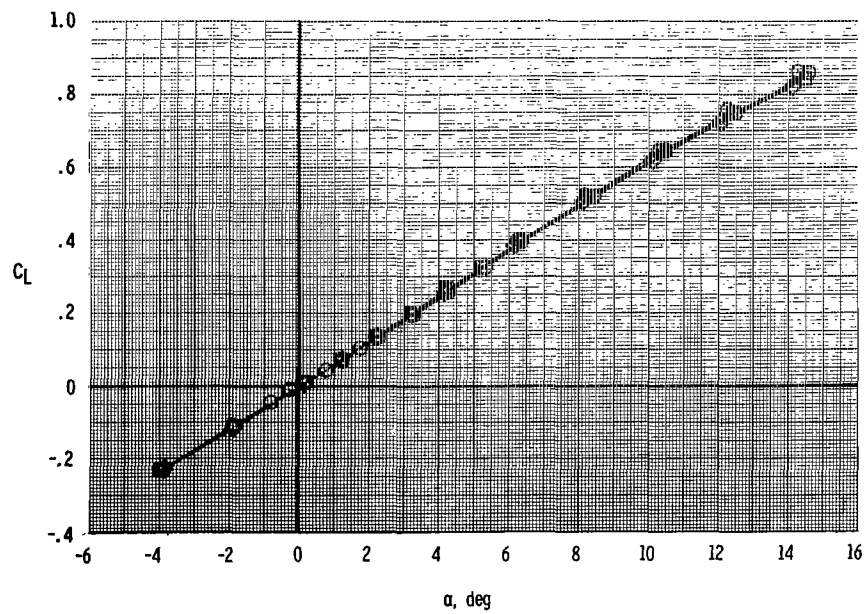
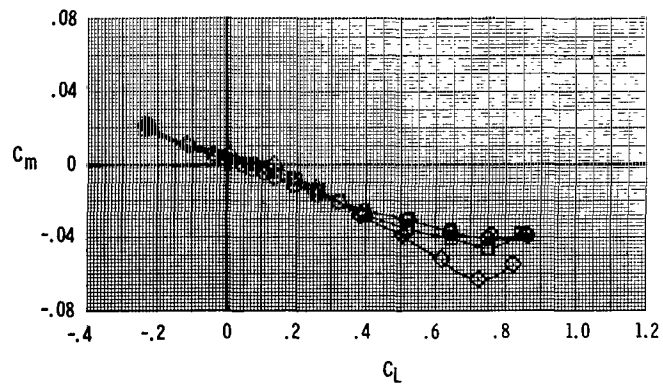


$\delta_c$ deg	
Left	Right
○	0
□	5
◇	10



(a)  $M = 0.40$ .

Figure 6.- Effect of differential canard-panel deflection on model longitudinal aerodynamic coefficients.



(b)  $M = 0.60$ .

Figure 6.- Continued.

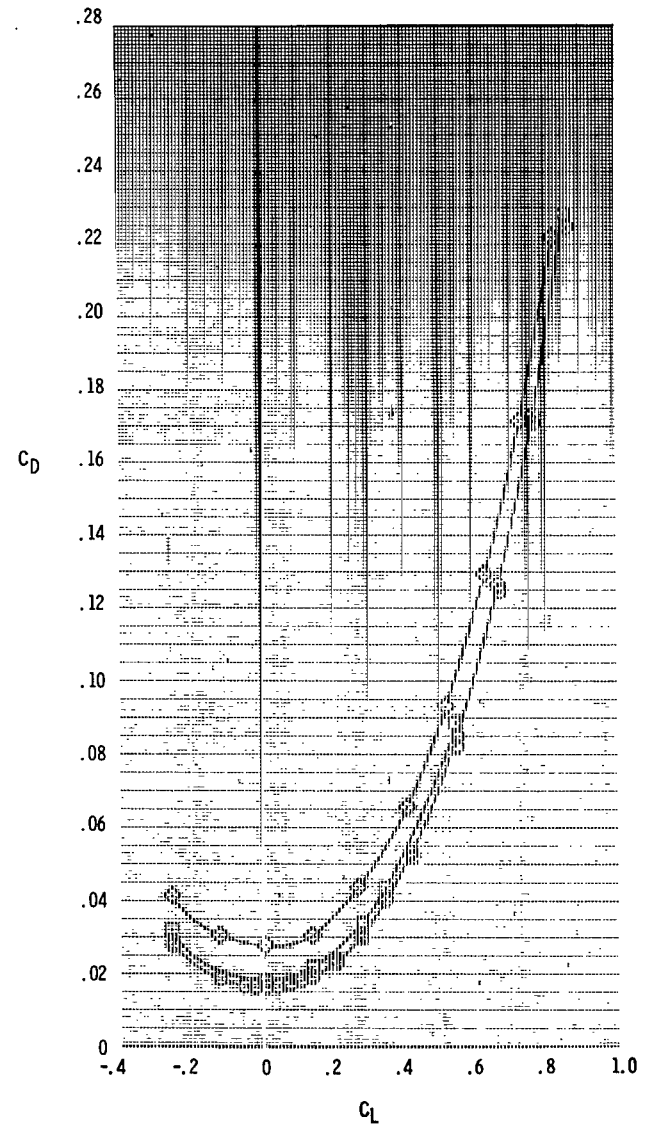
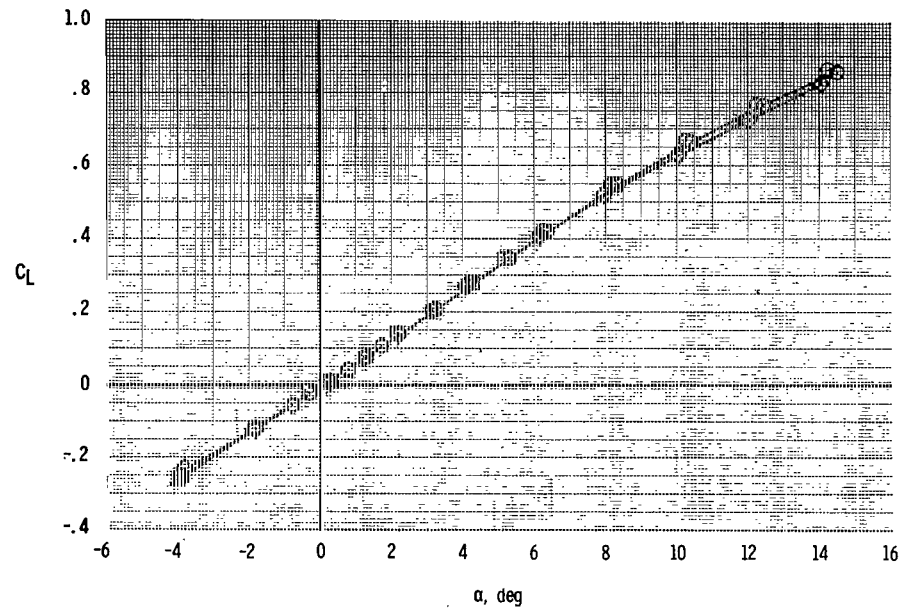
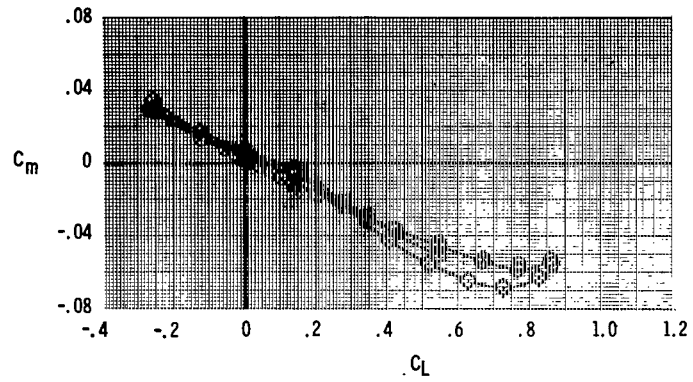
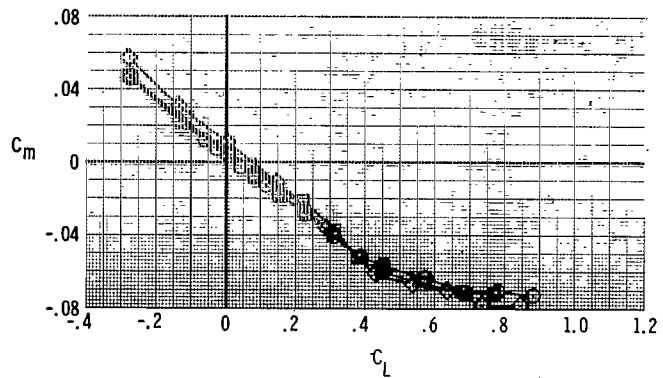
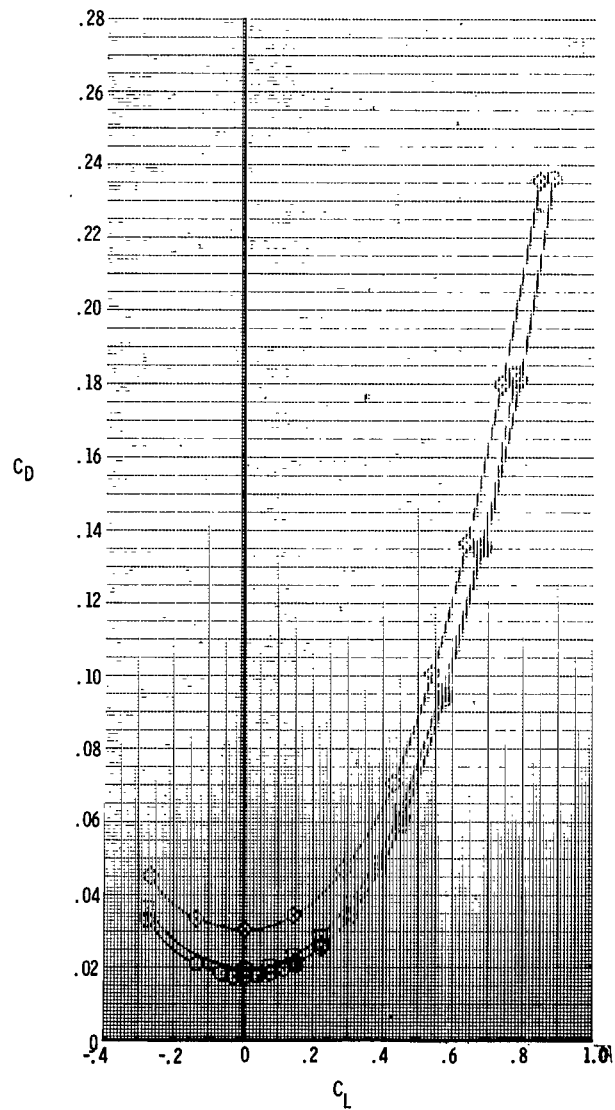
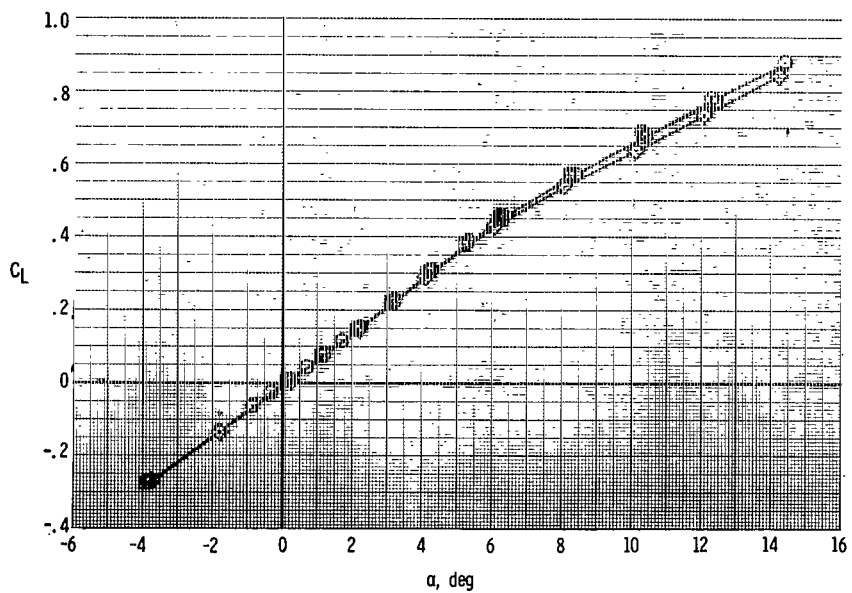
(c)  $M = 0.80$ .

Figure 6.- Continued.

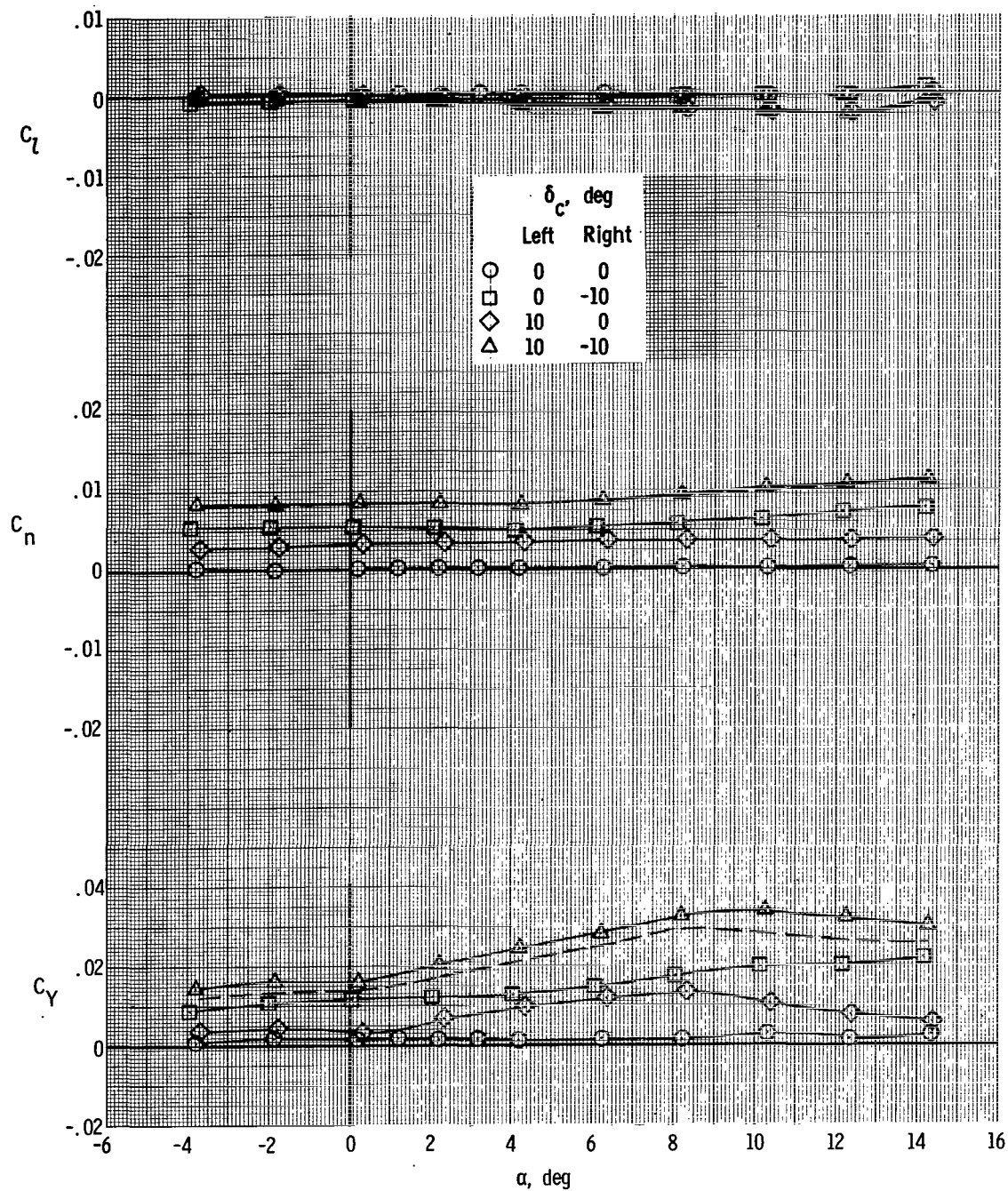


$\delta_c$ , deg	
Left	Right
○	0
□	5
◇	10



(d)  $M = 0.90$ .

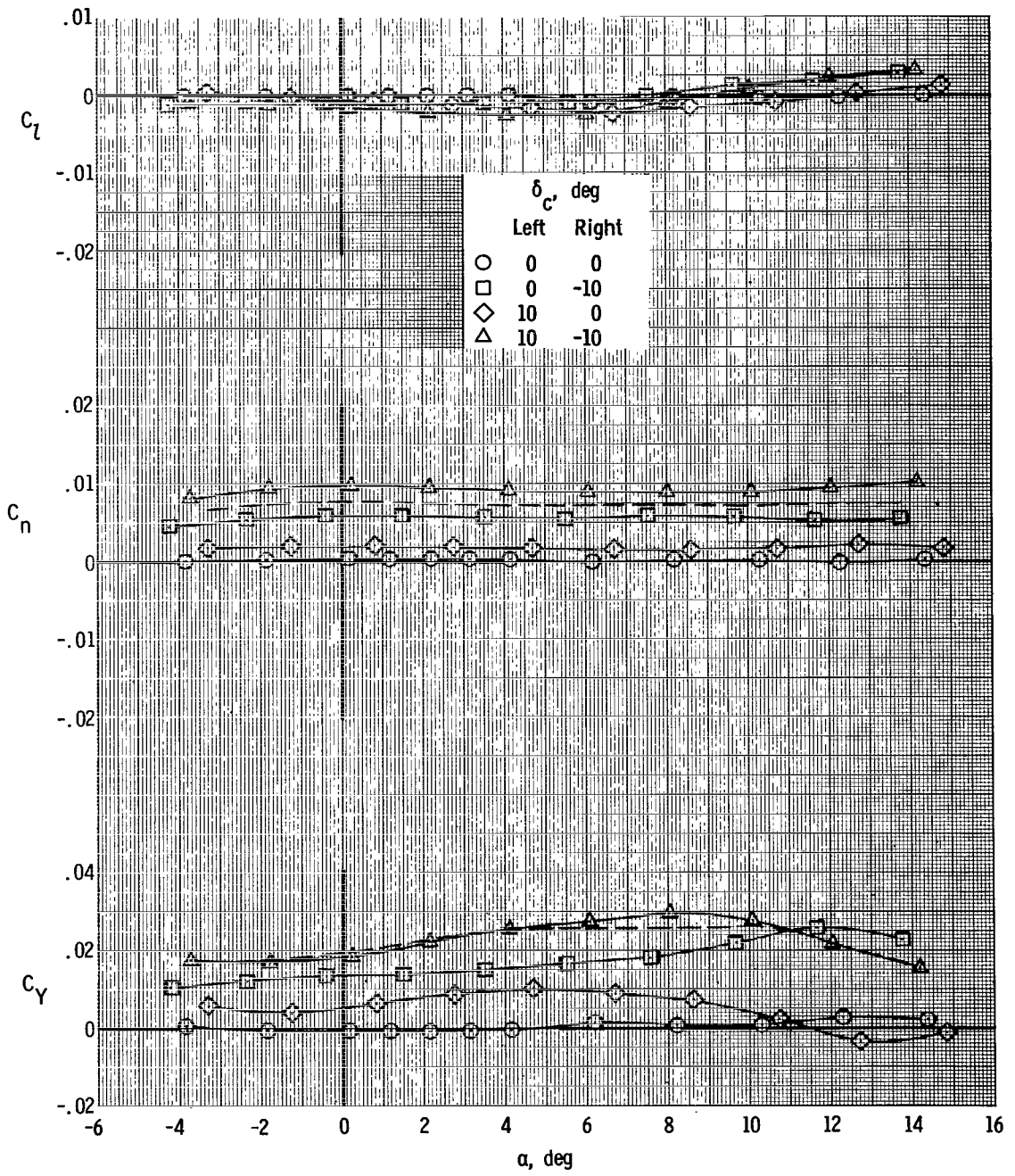
Figure 6.- Concluded.



(a)  $M = 0.40$ .

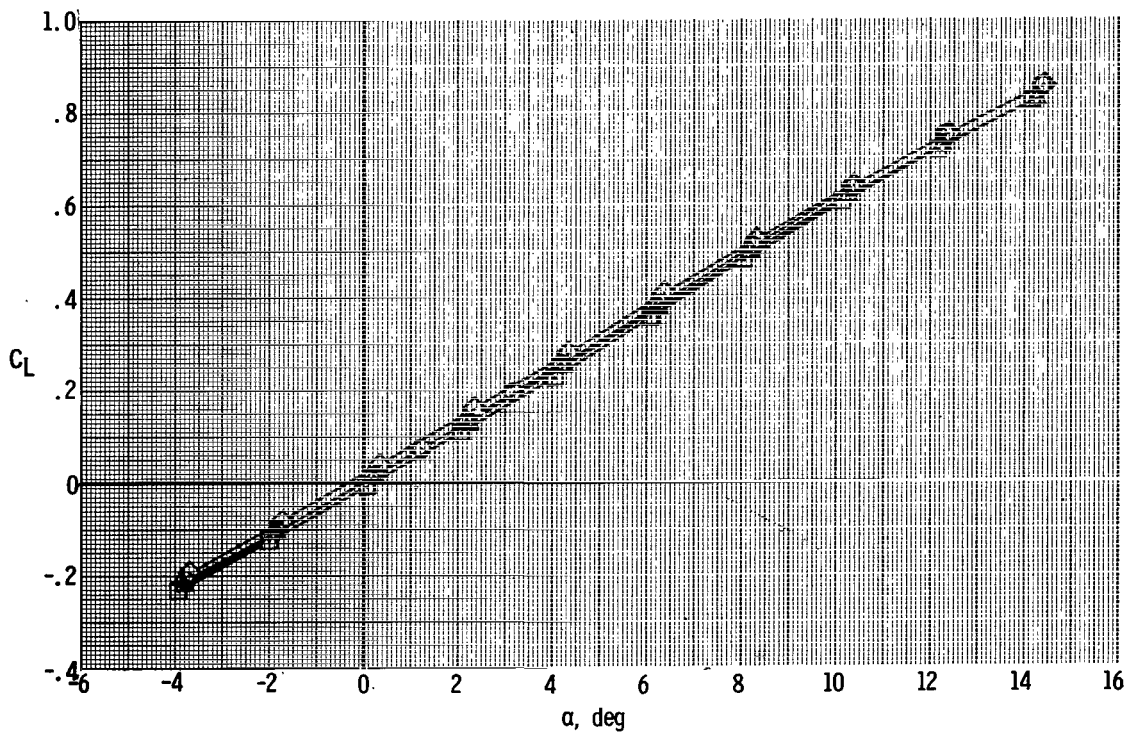
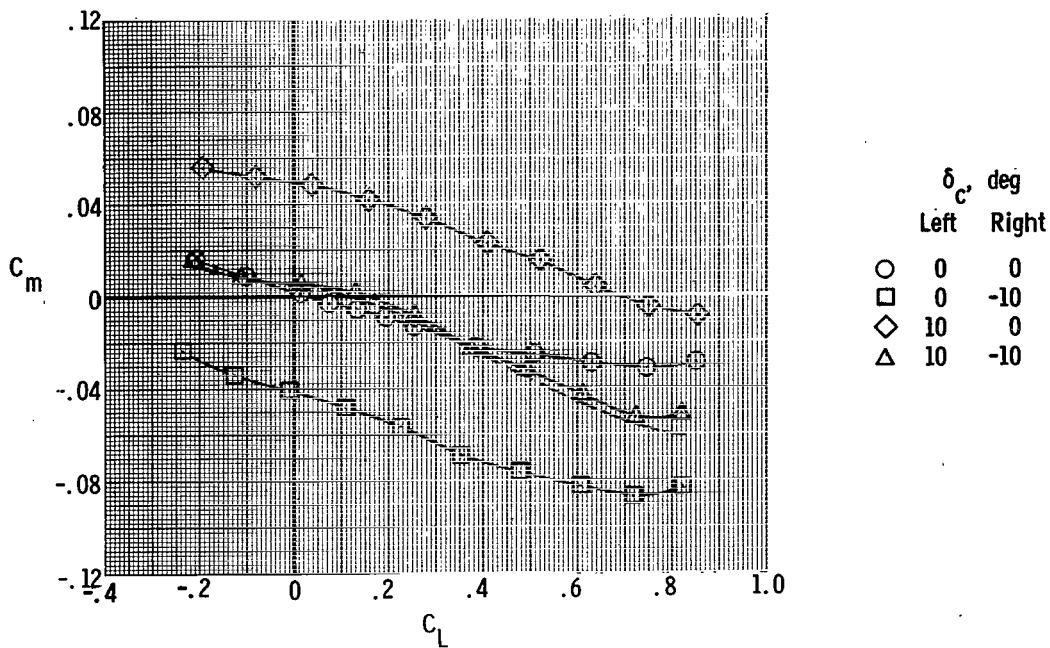
Figure 7.- Effect of differential and single canard-panel deflection on model lateral aerodynamic coefficients. Dashed lines indicate sums of side-force and yawing-moment increments due to single panel deflection.





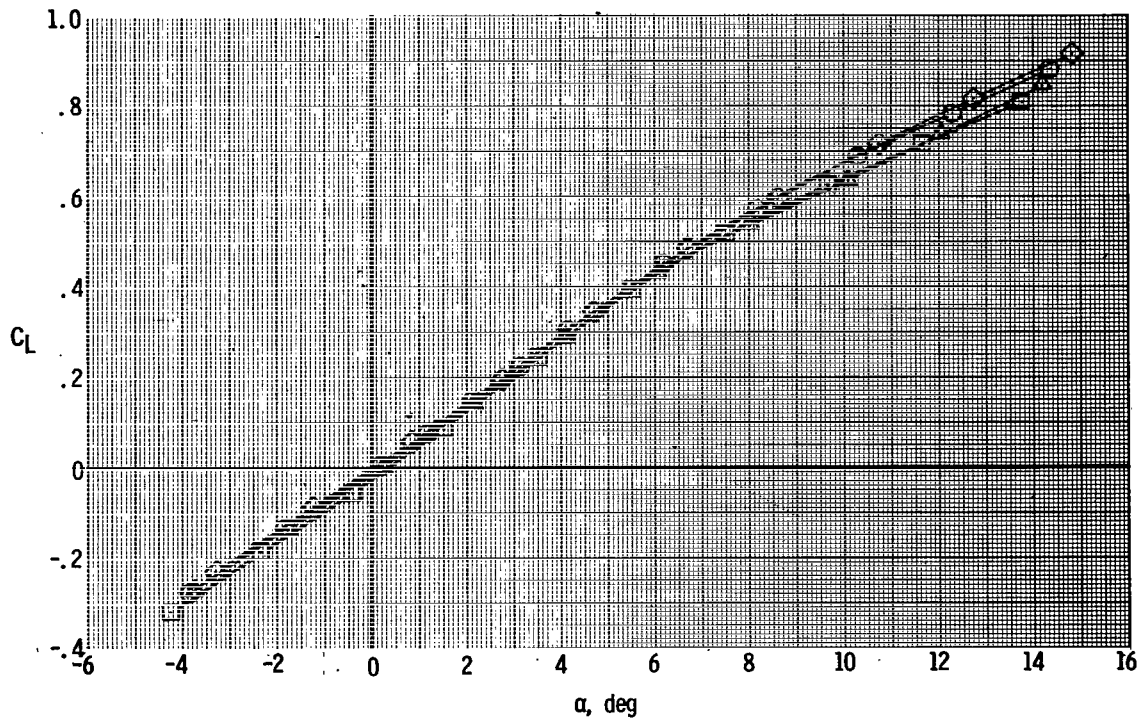
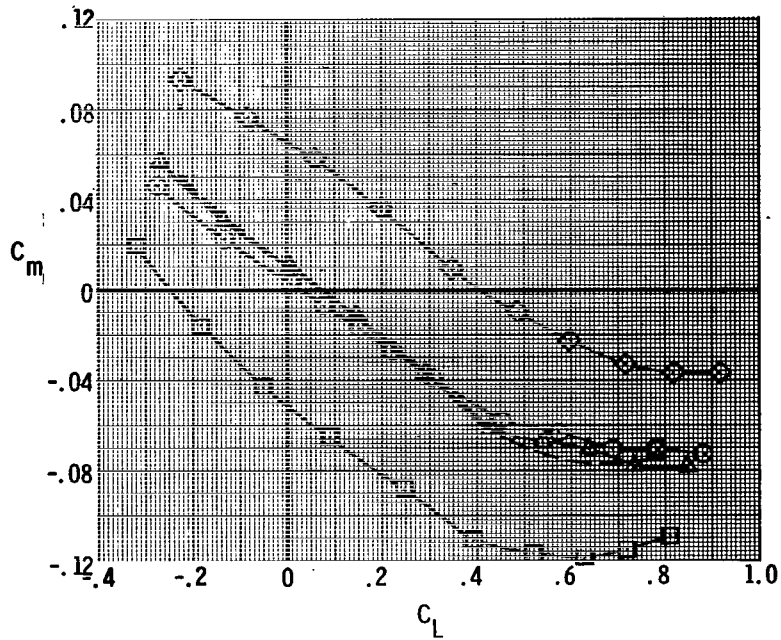
(b)  $M = 0.90$ .

Figure 7.- Concluded.



(a)  $M = 0.40$ .

Figure 8.- Effect of differential and single canard-panel deflection on model lift and pitching-moment characteristics. Dashed lines indicate sum of pitching-moment increments due to single panel deflection.



(b)  $M = 0.90$ .

Figure 8.- Concluded.

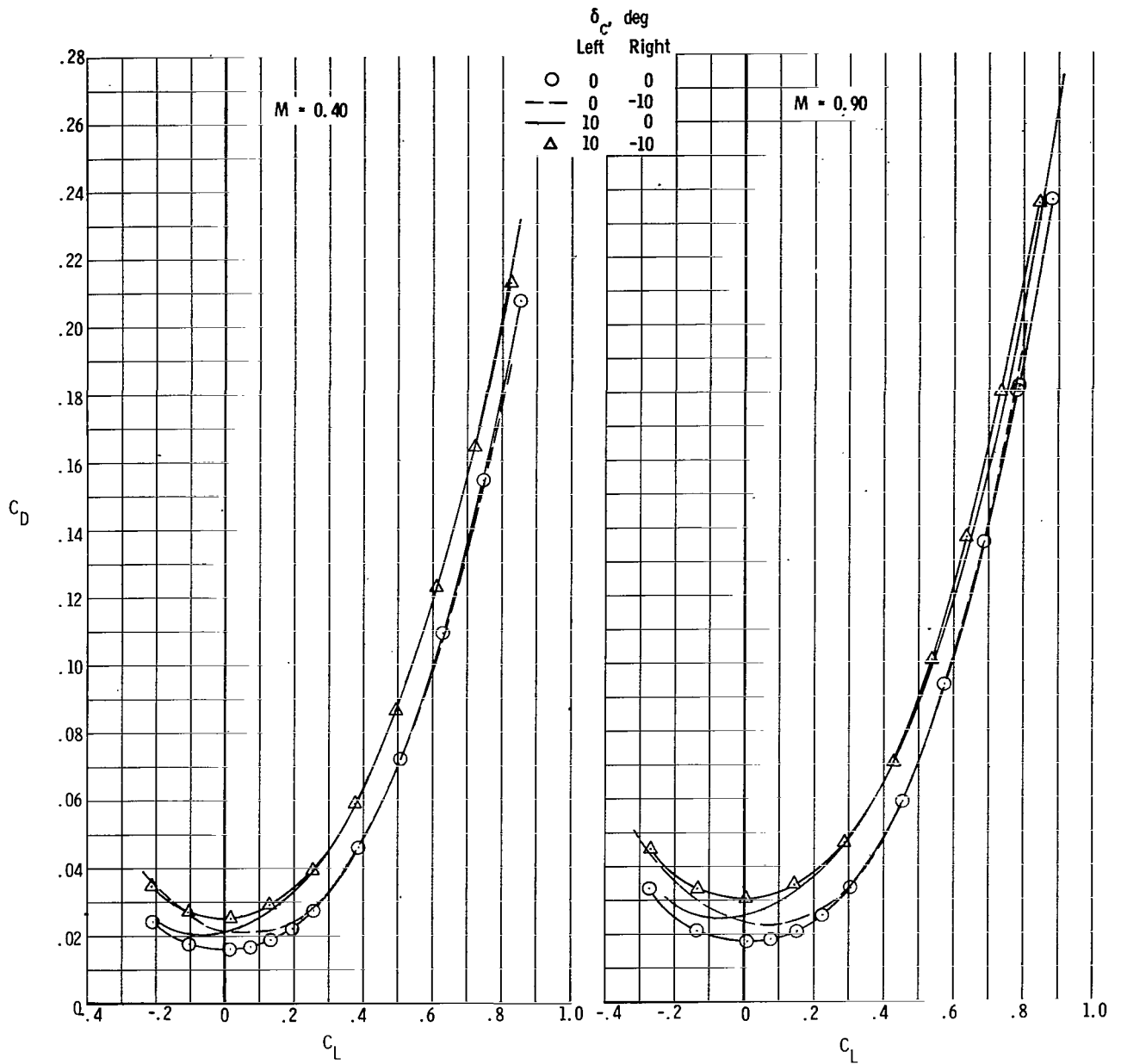
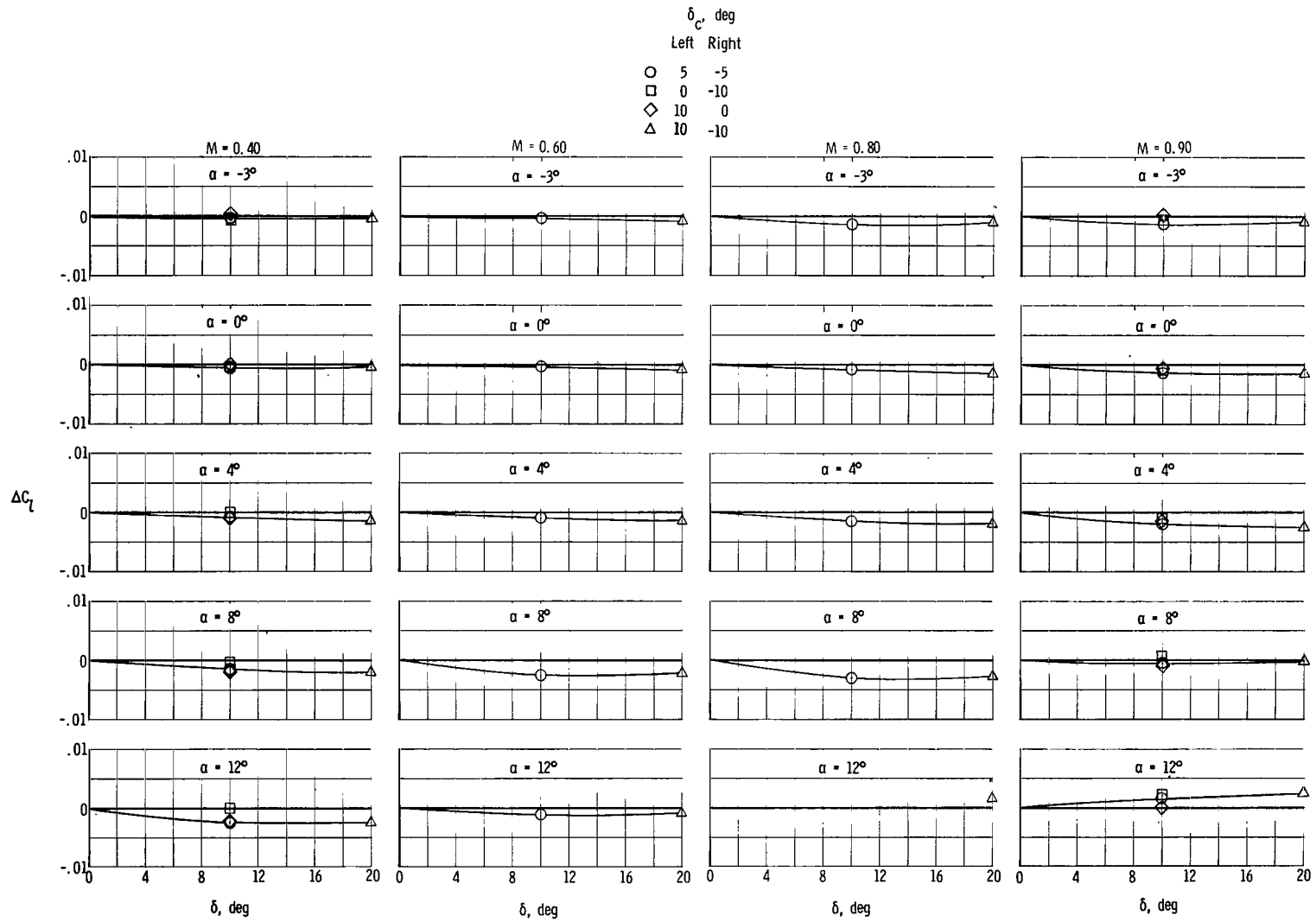
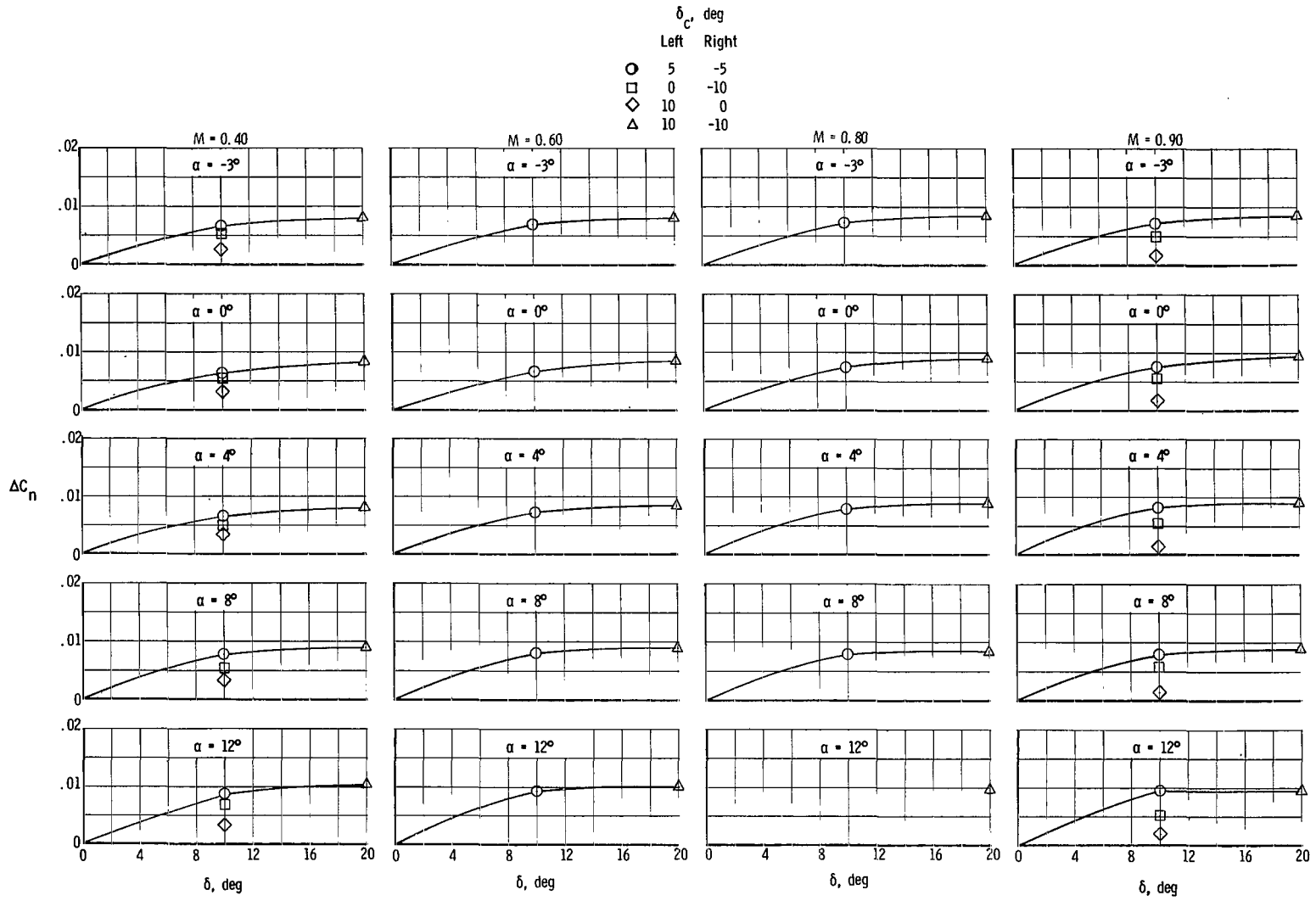


Figure 9.- Effect of differential and single canard-panel deflection on model drag coefficient.



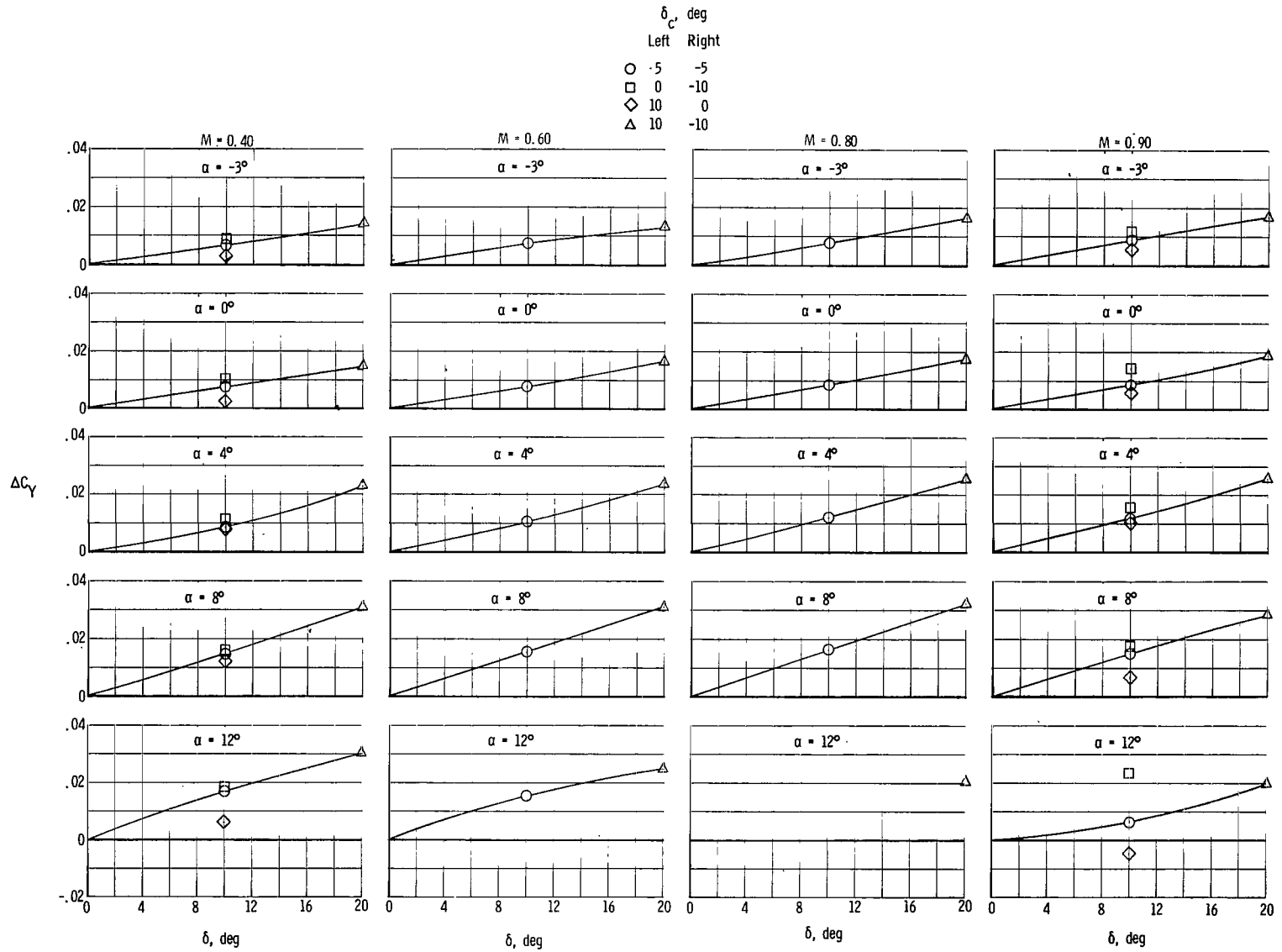
(a)  $\Delta C_l$ .

Figure 10.- Variation with total canard deflection angle of aerodynamic-coefficient increments due to differential and single canard-panel deflection.



(b)  $\Delta C_n$ .

Figure 10.- Continued.



(c)  $\Delta C_Y$ .

Figure 10.- Continued.

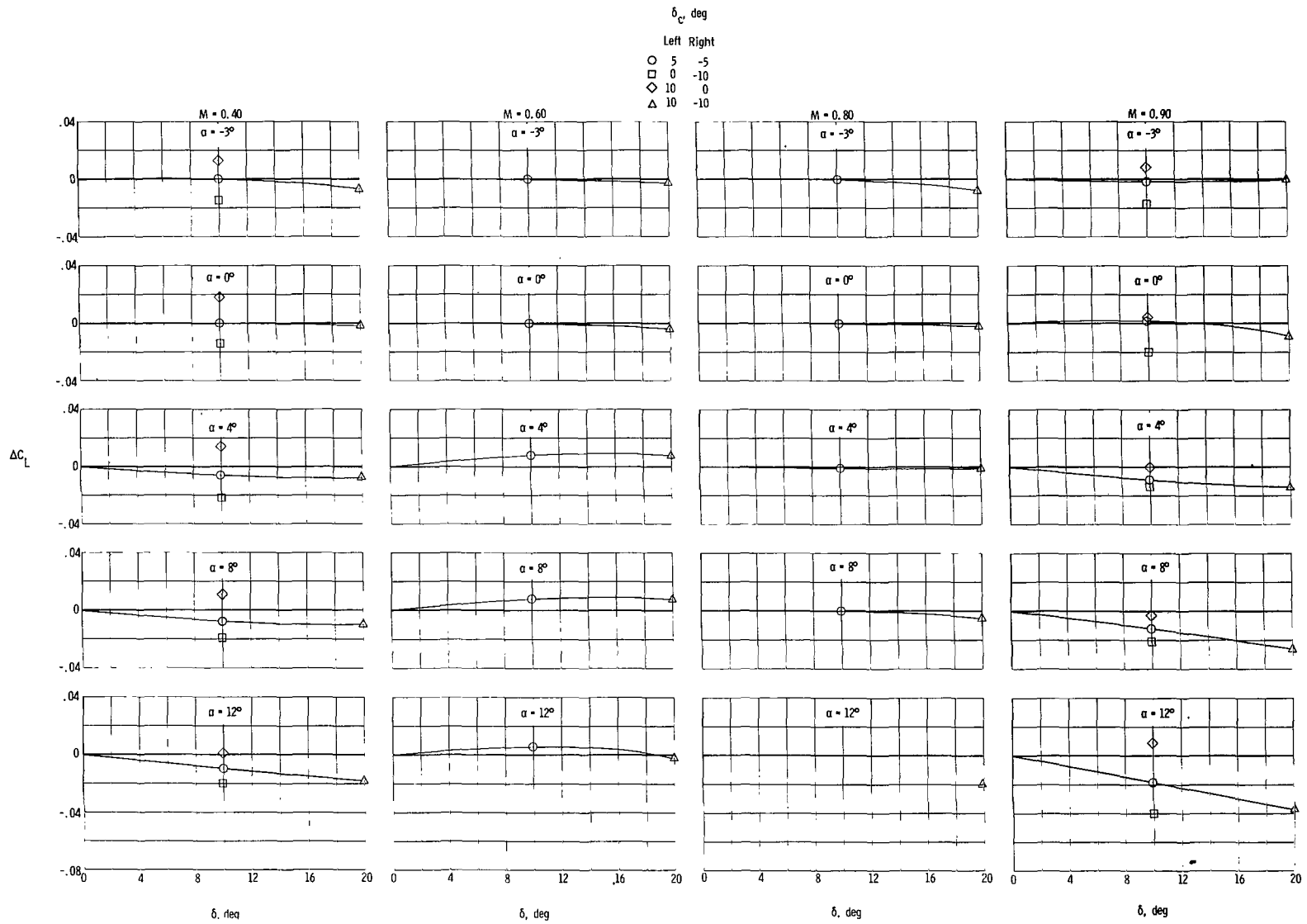
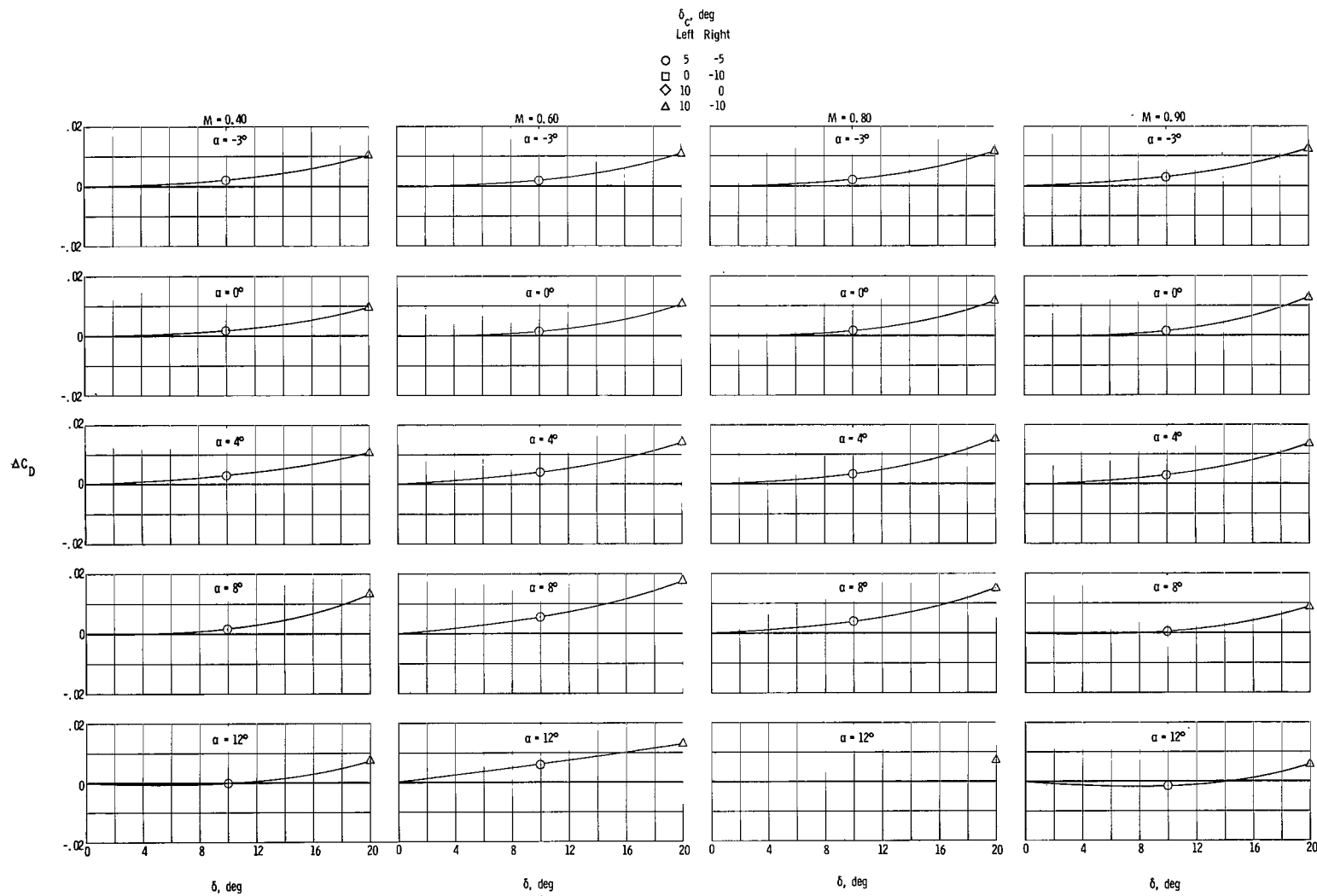
(d)  $\Delta C_L$ .

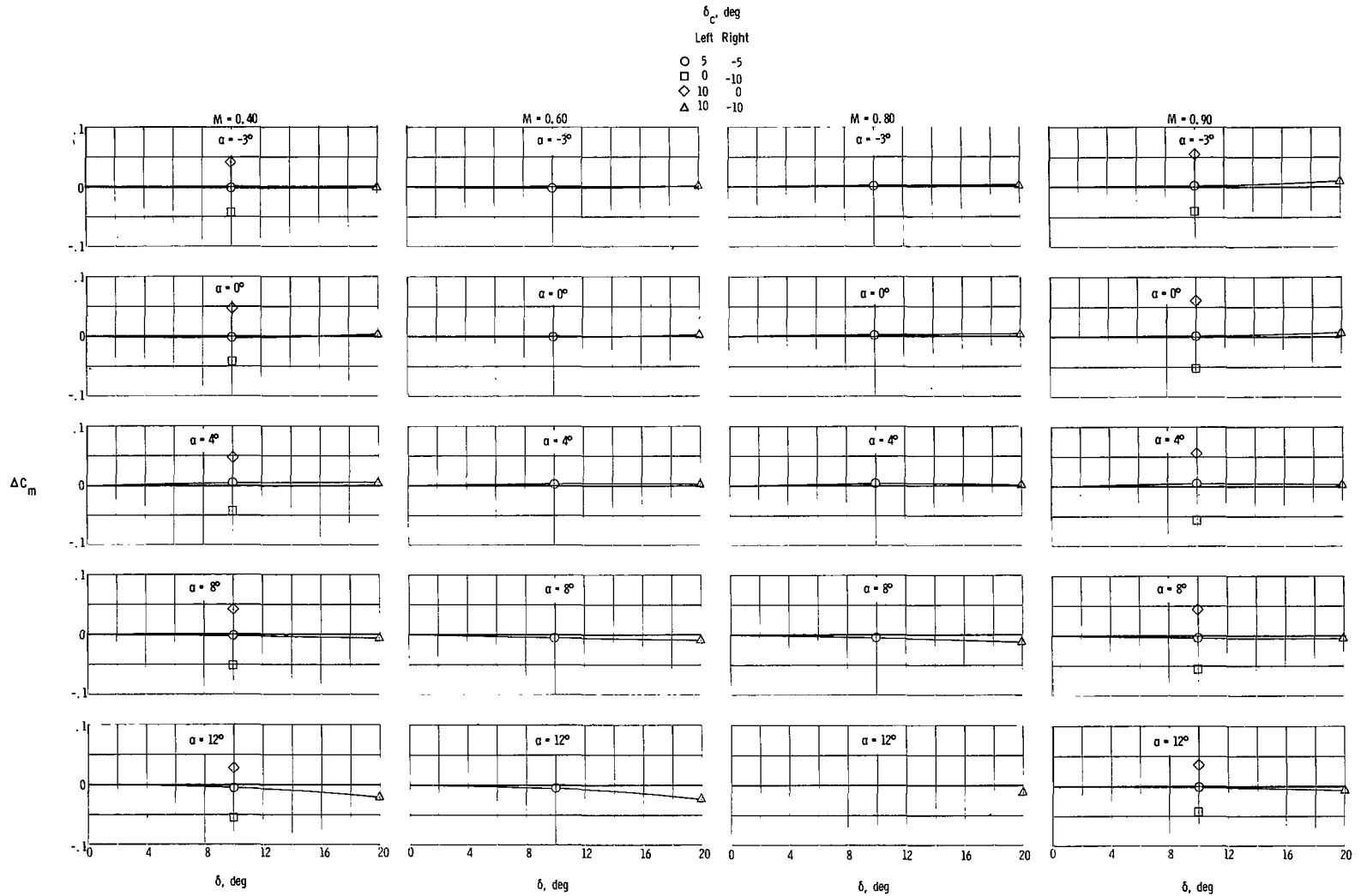
Figure 10.- Continued.





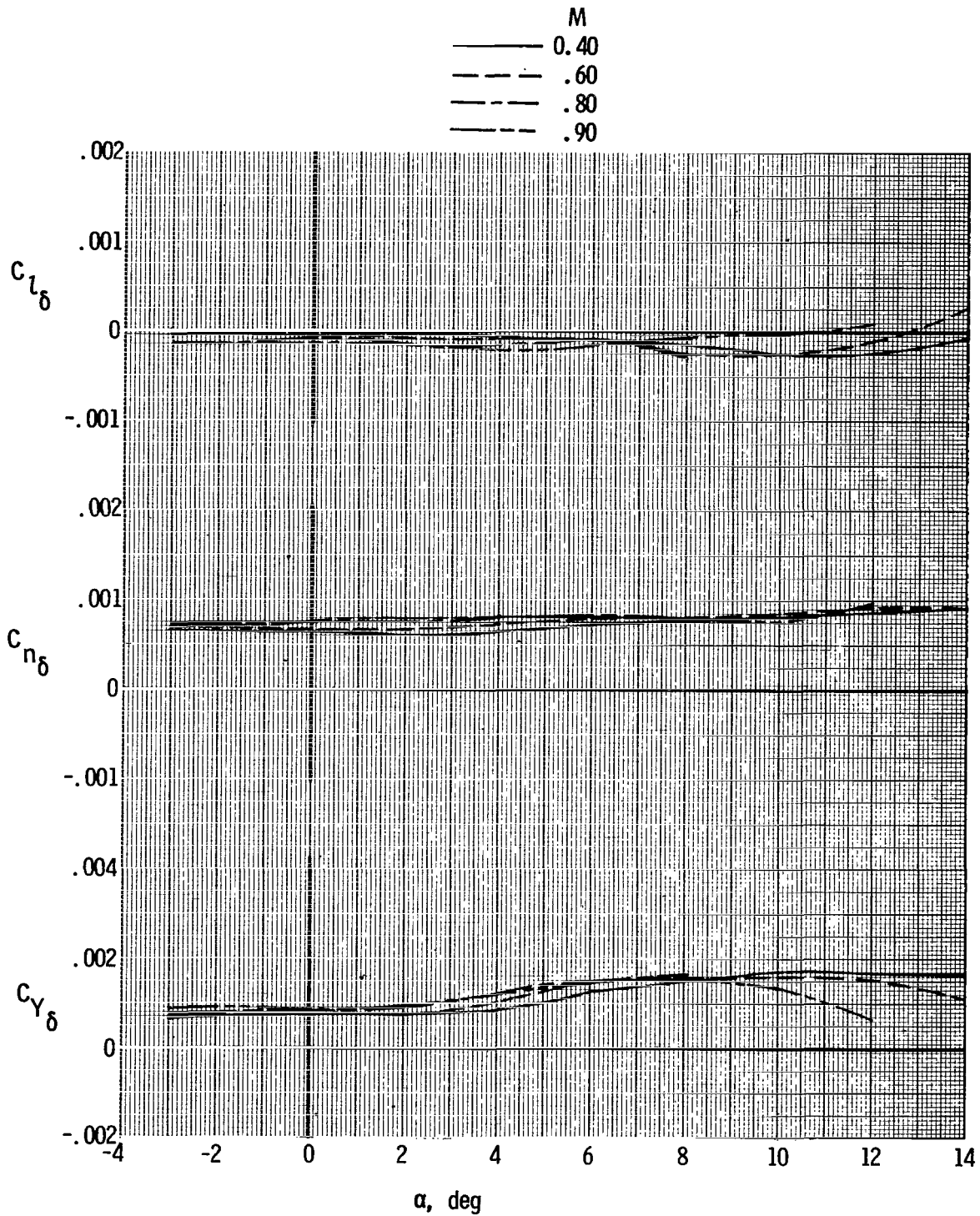
(e)  $\Delta C_D$ .

Figure 10.- Continued.



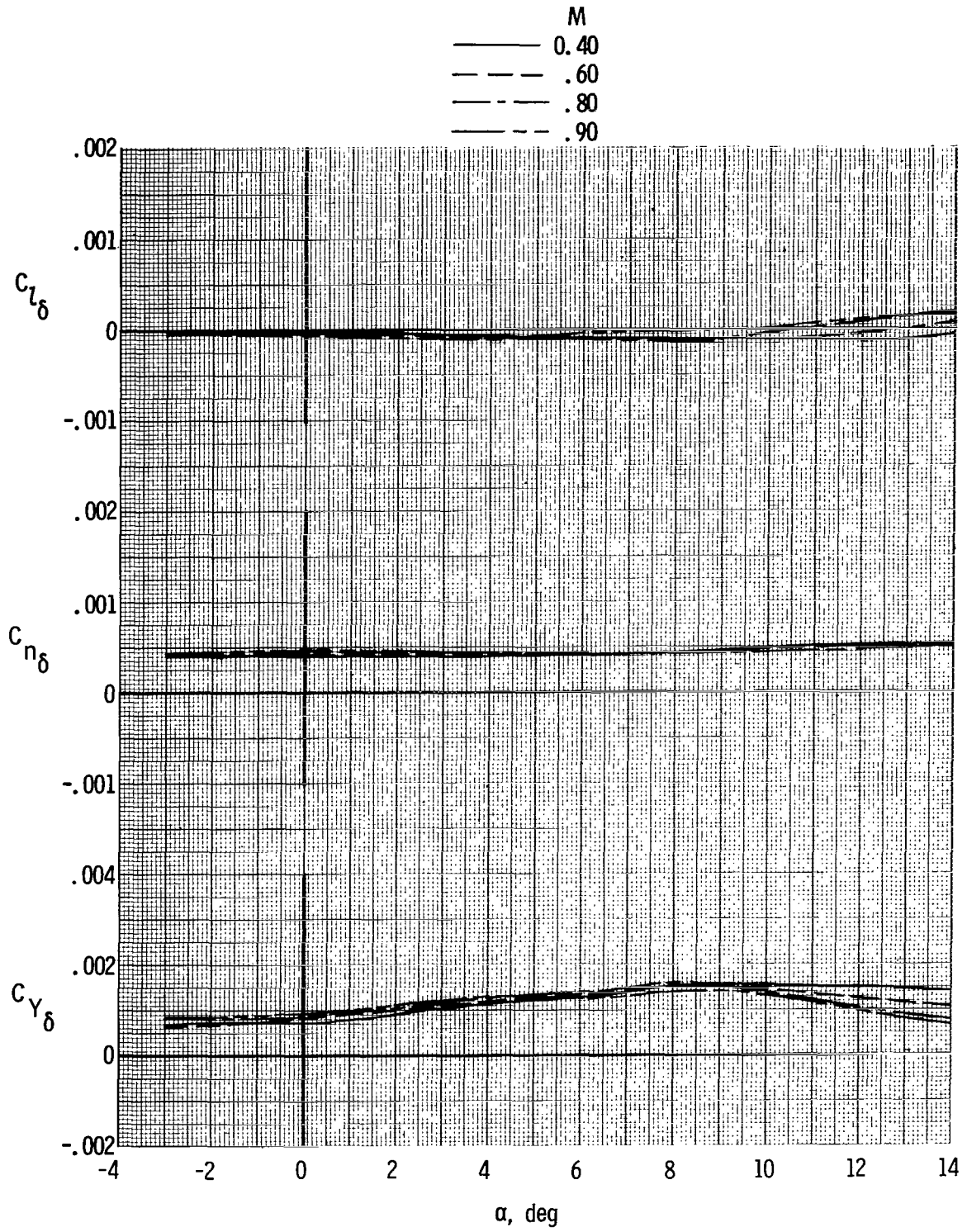
(f)  $\Delta C_m$ .

Figure 10.- Concluded.



(a)  $\delta_{c,Left} = 5^{\circ}$  and  $\delta_{c,Right} = -5^{\circ}$ .

Figure 11.- Variation with angle of attack of model lateral aerodynamic characteristics due to differential canard-panel deflection.



(b)  $\delta_{c,Left} = 10^\circ$  and  $\delta_{c,Right} = -10^\circ$ .

Figure 11.- Concluded.

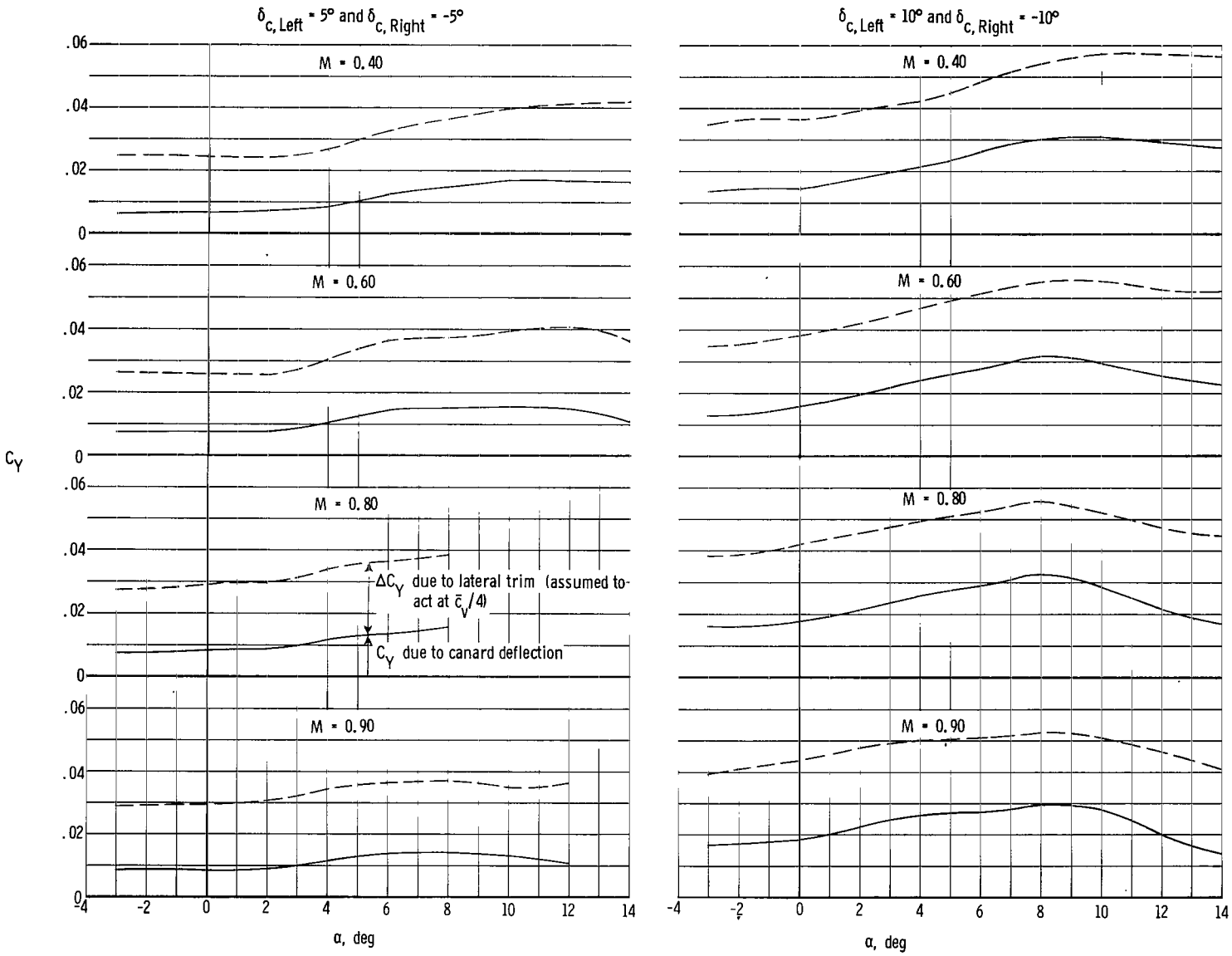


Figure 12.- Variation with angle of attack of trimmed (calculated) side-force coefficient.

NATIONAL AERONAUTICS AND SPACE ADMINISTRATION  
WASHINGTON, D.C. 20546

OFFICIAL BUSINESS  
PENALTY FOR PRIVATE USE \$300

SPECIAL FOURTH-CLASS RATE  
BOOK

POSTAGE AND FEES PAID  
NATIONAL AERONAUTICS AND  
SPACE ADMINISTRATION  
451



502 001 C1 U A 770708 S00903DS  
DEPT OF THE AIR FORCE  
AF WEAPONS LABORATORY  
ATTN: TECHNICAL LIBRARY (SUL)  
KIRTLAND AFB NM 87117

POSTMASTER: If Undeliverable (Section 158  
Postal Manual) Do Not Return

*"The aeronautical and space activities of the United States shall be conducted so as to contribute . . . to the expansion of human knowledge of phenomena in the atmosphere and space. The Administration shall provide for the widest practicable and appropriate dissemination of information concerning its activities and the results thereof."*

—NATIONAL AERONAUTICS AND SPACE ACT OF 1958

## NASA SCIENTIFIC AND TECHNICAL PUBLICATIONS

**TECHNICAL REPORTS:** Scientific and technical information considered important, complete, and a lasting contribution to existing knowledge.

**TECHNICAL NOTES:** Information less broad in scope but nevertheless of importance as a contribution to existing knowledge.

**TECHNICAL MEMORANDUMS:** Information receiving limited distribution because of preliminary data, security classification, or other reasons. Also includes conference proceedings with either limited or unlimited distribution.

**CONTRACTOR REPORTS:** Scientific and technical information generated under a NASA contract or grant and considered an important contribution to existing knowledge.

**TECHNICAL TRANSLATIONS:** Information published in a foreign language considered to merit NASA distribution in English.

**SPECIAL PUBLICATIONS:** Information derived from or of value to NASA activities. Publications include final reports of major projects, monographs, data compilations, handbooks, sourcebooks, and special bibliographies.

**TECHNOLOGY UTILIZATION PUBLICATIONS:** Information on technology used by NASA that may be of particular interest in commercial and other non-aerospace applications. Publications include Tech Briefs, Technology Utilization Reports and Technology Surveys.

*Details on the availability of these publications may be obtained from:*

**SCIENTIFIC AND TECHNICAL INFORMATION OFFICE**

**NATIONAL AERONAUTICS AND SPACE ADMINISTRATION**

**Washington, D.C. 20546**